

The Apoptotic Function Analysis of p53, Apaf1, Caspase3 and Caspase7 during the Spermatogenesis of the Chinese Fire-Bellied Newt *Cynops orientalis*

Da-Hui Wang^{1,9}, Jian-Rao Hu^{2,9}, Li-Ya Wang³, Yan-Jun Hu³, Fu-Qing Tan⁴, Hong Zhou¹, Jian-Zhong Shao¹, Wan-Xi Yang^{1*}

1 The Sperm Laboratory, College of Life Sciences, Zhejiang University, Hangzhou, People's Republic of China, **2** College of Life and Environmental Sciences, Hangzhou Normal University, Hangzhou, People's Republic of China, **3** Department of Reproductive Endocrinology, The Women's Hospital, School of Medicine, Zhejiang University, Hangzhou, People's Republic of China, **4** The First Affiliated Hospital, College of Medicine, Zhejiang University, Hangzhou, People's Republic of China

Abstract

Background: Spontaneous and stress-induced germ cell apoptosis during spermatogenesis of multicellular organisms have been investigated broadly in mammals. Spermatogenetic process in urodele amphibians was essentially like that in mammals in spite of morphological differences; however, the mechanism of germ cell apoptosis in urodele amphibians remains unknown. The Chinese fire-belly newt, *Cynops orientalis*, was an excellent organism for studying germ cell apoptosis due to its sensitiveness to temperature, strong endurance of starvation, and sensitive skin to heavy metal exposure.

Methodology/Principal Findings: TUNEL result showed that spontaneous germ cell apoptosis took place in normal newt, and severe stress-induced apoptosis occurred to spermatids and sperm in response to heat shock (40°C 2 h), cold exposure (4°C 12 h), cadmium exposure (Cd 36 h), and starvation stress. Quantitative reverse transcription polymerase chain reactions (qRT-PCR) showed that gene expression of *Caspase3* or *Caspase7* was obviously elevated after stress treatment. *Apaf1* was not altered at its gene expression level, and *p53* was significantly decreased after various stress treatment. Caspase assay demonstrated that Caspase-3, -8, -9 enzyme activities in newt testis were significantly elevated after heat shock (40°C 2 h), cold exposure (4°C 12 h), and cadmium exposure (Cd 36 h), while Caspase3 and Caspase8 activities were increased with Caspase9 significantly decreased after starvation treatment.

Conclusions/Significance: Severe germ cell apoptosis triggered by heat shock, cold exposure, and cadmium exposure was Caspase3 dependent, which probably involved both extrinsic and intrinsic pathways. Apaf1 may be involved in this process without elevating its gene expression. But starvation-induced germ cell apoptosis was likely mainly through extrinsic pathway. p53 was probably not responsible for stress-induced germ cell apoptosis in newt testis. The intriguing high occurrence of spermatid and sperm apoptosis probably resulted from the sperm morphology and unique reproduction policy of Chinese fire-belly newt, *Cynops orientalis*.

Citation: Wang D-H, Hu J-R, Wang L-Y, Hu Y-J, Tan F-Q, et al. (2012) The Apoptotic Function Analysis of p53, Apaf1, Caspase3 and Caspase7 during the Spermatogenesis of the Chinese Fire-Bellied Newt *Cynops orientalis*. PLoS ONE 7(6): e39920. doi:10.1371/journal.pone.0039920

Editor: Sue Cotterill, St. Georges University of London, United Kingdom of America

Received: February 13, 2012; **Accepted:** May 29, 2012; **Published:** June 29, 2012

Copyright: © 2012 Wang et al. This is an open-access article distributed under the terms of the Creative Commons Attribution License, which permits unrestricted use, distribution, and reproduction in any medium, provided the original author and source are credited.

Funding: This work was supported in part by the following projects: National Natural Science Foundation of China (No. 31072198 and 81100393), the National Basic Research Program of China (973 Program, Grant number: No. 2012CB967902), Zhejiang Provincial Natural Science Foundation of China (No. Y2100296). The funders had no role in study design, data collection and analysis, decision to publish, or preparation of the manuscript.

Competing Interests: The authors have declared that no competing interests exist.

* E-mail: wxyang@spermlab.org

⁹ These authors contributed equally to this work.

Introduction

Apoptosis is evolutionarily conserved, genetically driven and energy-dependent programmed cell death, which plays pivotal roles in development and homeostasis of multicellular organisms [1,2]. A large body of evidence proved the great importance of apoptosis for spermatogenesis in vertebrates and invertebrates [3,4,5,6,7,8]. Spermatogenesis is a well-organized complex process, in which diploid spermatogonia proliferate and differentiate into terminally haploid mature functional sperm. However, during normal spermatogenesis not all spermatogonia in the testis can undergo spermiogenesis and become mature sperm, for most of them are eliminated through spontaneous germ cell apoptosis

[7,8,9]. Notably, germ cell apoptosis can be induced by various environmental or physiological stress, such as heat shock, UV irradiation, toxicant exposure, hormonal withdrawal and oxidative stress [3,10,11,12,13,14,15,16]. Both spontaneous apoptosis and stress-induced apoptosis are indispensable for healthy germ cell development and functional sperm maturation [17]. Above all, apoptosis maintains cellular homeostasis and a suitable ratio of Sertoli cells to germ cell. Furthermore, apoptosis serves to eliminate potentially defective germ cells and ensure high-quality gametes production [18,19,20]. Finally, apoptosis keeps germline genetic integrity by clearing off mutant cells and prevents transmission of mutations to progeny and offspring [21,22,23].

Two different mechanisms have been elucidated for cell apoptosis: the extrinsic receptor-mediated pathway and the intrinsic mitochondria-dependent pathway. The extrinsic pathway was initiated with the extracellular death ligands, like Fas ligand (FasL), binding to their corresponding cell-surface receptors such as Fas. Then a death-inducible signaling complex (DISC) formed, leading to the activation of caspase8. Eventually, the activated caspase8 triggered activation of downstream effector caspases: caspase3, 6 and 7 that were directly responsible for cell demise [24,25,26]. By contrast, the intrinsic pathway was mainly regulated by Bcl-2 family members including Bax, Bak, Bcl-2, Bcl-xl and so on [21], which could positively or negatively regulate mitochondrial outer membrane permeabilization to promote the release of cytC (cytochrome C) and other apoptotic molecules. In cytosol, cytC, Apaf1 and procaspase9 were assembled into apoptosome to activate downstream effector caspase3, 6 and 7, leading to cellular components degradation and cell death [25]. Both the extrinsic and intrinsic pathways proved to participate in germ cell apoptosis during spermatogenesis. On the one hand, Bax-mediated apoptosis was indispensable for spermatogenesis [21]. Bax was elucidated to be essential for the progression of the first wave of spermatogenesis in mice [27], and it was found highly expressed in testis of young mice but only expressed at low level in spermatogonia of adult mice [28,29]. The Bax-null male mice were infertile as a result of disordered germ cell apoptosis, which caused excessive numbers of spermatogonia and pre-leptotene spermatocytes in spermatogenesis [13,21,30]. On the other hand, Fas and FasL were also evidenced essential for germ cell apoptosis during spermatogenesis. Fas was expressed in germ cells and FasL detected in Sertoli cells [31,32,33,34]. Testicular Fas participated in germ cell apoptosis triggered by testosterone withdrawal [35], UV radiation [36] and toxicants exposure [32,36].

Both the two distinct caspase-mediated apoptosis pathways could be regulated by p53. p53 was the most prominent tumor suppressor, and many types of cancers resulted from functionally impaired p53 [37,38] that lost its capability in DNA repairing and cell apoptosis induction. It was demonstrated that p53 played critical functions in germ cell apoptosis both through extrinsic pathway and intrinsic pathway, since it could regulate not only Bax, Bid, Bcl-2, Bcl-xL, Puma, Noxa, Apaf1 and IAP, but also death receptors like CD95, Fas, Apo-1 and DR5 [39,40,41,42,43,44]. p53-mediated apoptosis was found responsible for the initial phase of germ cell apoptosis during spermatogenesis in cryptorchid mice [31,45,46]. Moreover, under genotoxic stress, p53 was involved in apoptosis of spermatogonia, spermatocytes and spermatids [39,40,41]. A higher percentage of morphologically abnormal spermatozoa in the ejaculate and reduced fertility occurred to *p53*^{-/-} mice, which was probably due to failed germ cell apoptosis [45].

Previous researches on germ cell apoptosis mainly focused on mammals for an elaborate and comprehensive knowledge of mammalian spermatogenesis. Actually, the spermatogenic process in urodele amphibians is essentially like that in mammals in spite of morphological differences. During the spermatogenesis of *Cynops orientalis*, spermatogonia underwent several cycles of cell division to become spermatid, and later in spermiogenesis, the spermatid eventually matured into sperms. Mature sperm commonly contained typical acrosome, long and narrow nucleus and long flagellum, and a large number of mitochondria were arranged around the midpiece of the sperm flagellum. Like other newt species, the testis of *Cynops orientalis* consists of lobules in successive zones, and spermatogenesis proceeds synchronously in

these zones. Therefore, it is easy to isolate and identify germ cells of particular spermatogenic stage, which is very suitable for germ cell apoptosis analysis (unpublished data). As an important urodele amphibian, the Chinese fire-belly newts, *Cynops orientalis*, is an excellent organism for studying germ cell apoptosis due to its advantageous physiological features: sensitiveness to temperature, strong endurance of starvation and sensitive skin to environmental heavy metal. Coincidentally, temperature, starvation and heavy metals are often utilized to investigate germ cell apoptosis. Besides, germ cell apoptosis have been reported in Japanese fire-belly newts and marbled newts, and some unidentified caspase was reported involved in germ cell apoptosis in Japanese fire-belly newts [47,48,49,50,51,52,53,54]. However, the detailed mechanism of germ cell apoptosis was not elucidated. In the present study, we investigated the germ cell apoptosis induced by heavy metal exposure, starvation and temperature stress in Chinese fire-belly newts, *Cynops orientalis*. We provided evidence that stress-induced germ cell apoptosis occurred by activating Caspase3 both through extrinsic pathway and intrinsic pathway. In addition, Apaf1 probably was involved in the stress-induced germ cell apoptosis, whereas p53 was not likely responsible for this process, which needs further investigation.

Materials and Methods

Animals and Sampling

This study didn't involve non-human primates. Research work was performed in full accordance to the requirement by 'Governing Regulation for the Use of Experimental Animals in Zhejiang Province' (Zhejiang Provincial Government Order No 263, released in August 27, 2009, effective from October 1, 2010) and 'Governing Regulation for the Use of Experimental Animals in Zhejiang University' (Zhejiang University Order No 1 (2009), released in November 24, 2009). Fire-belly newts used in this study were purchased from local pet market of Fuyang Mountainous Area. The use of this animal was approved by local review boards for ethics in College of Life Sciences, Zhejiang University.

Adult Chinese fire-belly newts, *Cynops orientalis*, were collected from Fuyang Mountainous Area (Hangzhou, China). Animals were kept in big aquatic tank in laboratory (12 h light:12 h darkness at 22±2°C. All the animals were anesthetized by placing them for 20 min in a solution of 0.1% MS222 (Sigma, St. Louis). Fresh samples of testis, liver, muscle, intestine and heart were dissected and stored at -80°C for total RNA extraction.

Full-length cDNA Cloning of *p53*, *Apaf1*, *Caspase3* and *Caspase7*

Total RNA from the testis of adult Chinese fire-belly newt, *Cynops orientalis*, was extracted using Trizol (Invitrogen, USA) according to the instruction book, and reverse transcription was performed using BioRT cDNA First Strand Synthesis Kit (Bioer, Japan). Degenerate primers were designed using CODEHOP program supplied by Blocks WWW Server (<http://blocks.fhrc.org/>) based on conserved protein sequence, and gene specific primers designed by Primer 5.0 and Oligo 6. All degenerate primers and gene specific primers used for cloning *p53*, *Apaf1*, *Caspase3* and *Caspase7* were presented in **Table 1** and **Table 2**. Polymerase chain reactions (PCR) were run in Mygene Series Peltier Thermal Cyclers (Hangzhou, China), and the PCR program for amplifying cDNA fragment was as follows: 94°C for 5 min, 15 cycles in a touch down program (94°C for 30 s, 55°C for 30 s and 72°C for 30 s, followed by a 0.5°C decrease of the annealing temperature per cycle), and then 32 cycles were

performed (30 s at 94°C, 30 s at 48°C and 30 s at 72°C) with 10 min at 72°C for the final extension. The RACE (Rapid amplification of cDNA ends) PCR were run according to Smart RACE cDNA Amplification Kit (ClonTech) and 3'Full RACE Amplification Kit (Takara). The target PCR products were cloned into pMD18-T vector (TaKaRa) and sequenced by Sangon Company (Shanghai, China).

Protein Alignment and Structure Prediction of p53, Apaf1, Caspase3 and Caspase7

The protein alignment and structure prediction were performed using Vector NTI10 (Invitrogen, USA) and online softwares (<http://www.expasy.org/tools/scanprosite/>) (<http://smart.embl-heidelberg.de/>) (<http://zhanglab.cmb.med.umich.edu/I-TASSER/>) [55,56,57]. The GenBank accession numbers of Apaf1 proteins in protein alignment are as follows: *Cynops orientalis* (JQ320086); *Homo sapiens* (O14727.2); *Mus musculus* (NP_033814.2); *Xenopus laevis* (NP_001085834.1); *Danio rerio* (NP_571683.1). The GenBank accession numbers of p53 proteins used are as follows: *Cynops orientalis* (HM627863); *Homo sapiens*(BAC16799.1); *Mus musculus* (BAA82343.1); *Xenopus laevis*(CAA54672.1); *Danio rerio* (NP_571402.1).The GenBank accession numbers of Caspase7 proteins used are as follows: *Cynops orientalis* (JQ320087); *Homo sapiens* (AAC50346.1); *Mus musculus*(BAA19730.1); *Xenopus laevis* (NP_001091272.1); *Danio rerio* (AAH95327.1). The GenBank accession numbers of Caspase3 proteins used are as follows: *Cynops orientalis* (JQ320088); *Danio*

Table 1. Primers used for the study of Caspase3 and Caspase7 in *Cynops orientalis*.

Primer name	Primer Sequence (5' to 3')	Usage
Csp AF1	ATTGTATTATTATAAaayaaraaytt	Caspase7/3 cloning
Csp BF2	AAGAAATGGAacngaygtnga	Caspase7/3 cloning
Csp DR2	GAATAAGCATACAGAAATCNGCYTCNAC	Caspase7/3 cloning
Csp CR1	CCTGAATGAAAAACAGTTTNGGYTTNCC	Caspase7/3 cloning
Csp CF1	ACCAAAACTGTTCTTTATTcargcntgymg	Caspase3 cloning
Csp3IF1	AAAGTTTTCAATGACCAAGC	Caspase3 cloning
Csp3IR1	ATCTGACGAATCTCCTCCAC	Caspase3 cloning
Csp7-3' gspF1	CTTATCTATGGACAGACGGGC	Caspase7-3' RACE
Csp7-3' gspF2	GGTGAAGAGGGACTTATCTATGGG	Caspase7-3' RACE
Csp7-5' gspR1	GCTGCTCCATTTCTCACAGGTCGGA	Caspase7-5' RACE
Csp7-5' gspR2	AGCAGGCATAATCACTGTGGTCTTCTT	Caspase7-5' RACE
Csp3-3' gspF1	ATCAACAGAGGATACCCGTGGA	Caspase3-3' RACE
Csp3-3' gspF2	GCAGACAGTGGAGGAGATTCTGT	Caspase3-3' RACE
Csp3-5' gspR1	GTAAGAAAACACTTCTGAGATTTGCGG	Caspase3-5' RACE
Csp3-5' gspR2	CCCAAGGTAAGAAAACACTTCTGAGAT	Caspase3-5' RACE
Csp7rIF1	TGGATGTTTATGTACACCTTTTC	Realtime PCR
Csp7rIR1	AGTCTATTTTATTATGGGCTCG	Realtime PCR
Csp3rIF1	AGAGAACAATGGCGGATA	Realtime PCR
Csp3rIR1	CCAGTTGAGGGATGAAAG	Realtime PCR

doi:10.1371/journal.pone.0039920.t001

Table 2. Primers used for the study of p53 and Apaf1 in *Cynops orientalis*.

Primers name	Primer Sequence(5' to 3')	Usage
P2F1	TGAGAAGATGTCCACAYCAYGARMG	p53 Cloning
P5R1	CAAGCACACTCKNACYTCRAA	p53 Cloning
P5R2	ATCTCTTCTGGACANGRCANAC	p53 Cloning
P5'-gspR3	CCTGCGGAGTCTCGTATGGACCAACAC	p53 5' RACE
P5'-gspR2	TGGCCACCAACACGCTGTGGCGACGGG	p53 5' RACE
P3'-gspF3	GCCACAGCGTGTGGTCCATACGAGAC	p53 3' RACE
P3'-gspF2	CGCCGACCAATCTGACTATCATTACAC	p53 3' RACE
P53RTF1	CCCCAAGAATGGCAAAAA	RT-PCR
P53RTR1	CCTGGCTCACCCACCTA	RT-PCR
p53rIF1	GATGACTGTCTCCACCCT	Realtime PCR
p53rIR1	TCTGCCTTGAATTCCTT	Realtime PCR
β-actinF	GAATCCCAAAGCCAACC	Realtime PCR/RT-PCR
β-actinR	CCAGCCAAGTCAAGACG	Realtime PCR/RT-PCR
Apaf2F	TTATGAAGCTCTGGAYGARGCNAT	Apaf1 cloning
Apaf4R2	TTTAAAAATCTGCAGTGTTRTCNGCNCC	Apaf1 cloning
Ap3'-gspF1	ATGCTTGCTTTTCCCTGATGG	Apaf1 3' RACE
Ap3'-gspF2	GTCCGCATACAGATGGAGTTTA	Apaf1 3' RACE
Ap5'-gspR1	GCATTTCTCCACCTCTTGTCTCCA	Apaf1 5' RACE
Ap5'-gspR2	GTGAGAAAATCCAGTTGAAGTCTGTGT	Apaf1 5' RACE
AprIF1	ATGGAGTTTATCATGCTTGC	Realtime-PCR/RT-PCR
AprIR1	CATAGGATTAGTCCGTTGG	Realtime-PCR/RT-PCR

doi:10.1371/journal.pone.0039920.t002

rerio (CAX14649.1); *Xenopus laevis* (NP_001081225.1); *Homo sapiens* (P42574); *Mus musculus* (P70677).

Analysis of tissue distribution of p53, Apaf1, Caspase3 and Caspase7 mRNA

Total RNA was extracted from muscle, heart, testis, intestine and liver using Trizol (Invitrogen, USA), and reverse transcription was performed using BioRT cDNA First Strand Synthesis Kit (Bioer, Japan). RT-PCR was used to analyze the gene expression level of *p53*, *Apaf1*, *Caspase3* and *Caspase7* in various tissues. The primers used for gene expression analysis were listed in Table 1 and Table 2, and the program was run as follows: 94°C for 5 min; 30 s at 94°C, 30 s at 60°C, and 30 s at 72°C (32 cycles); 10 min at 72°C for final extension. The β -actin served as the control, and the density of amplified bands were analyzed using Tanon GIS system (Tanon 2500).The gene expression levels of *p53*, *Apaf1*, *Caspase7* and *Caspase3* were presented as the ratio of their relative amount to β -actin transcripts.

Stress challenging the Testis of Chinese Fire-belly Newt, *Cynops orientalis*

Chinese fire-belly newts were initially raised in their best conditions and then divided into several groups for stress treatments that included cadmium exposure, heat shock, cold exposure and starvation. For cadmium exposure, newts were injected subcutaneously with cadmium chloride (CdCl_2) dissolved in saline (0.65% NaCl) according to the dosage of 50 mg/kg body weight. The newts in control group were injected only with 0.65% NaCl. Then these newts were raised for 12 h, 24 h and 36 h respectively at room temperature ($22 \pm 2^\circ\text{C}$). The newts for cold exposure were kept in the incubator at 4°C (4 h and 12 h) while the newts for heat shock were exposed to 38°C (2 h, 4 h and 12 h) and 40°C (2 h and 4 h). The newts raised at room temperature served as the control. For starvation treatment, the newts were starved for one month, and those with daily feed served as the control. In each stress group, all newts were recovered in normal conditions for 4 h before their testes dissection for RNA extraction and TUNEL analysis.

Analysis of Gene Expression of p53, Apaf1, Caspase3 and Caspase7 after Stress Treatment

Total RNA was extracted from the testes of stress-treated newts and control newts with Trizol (Invitrogen, USA). Reverse transcription was conducted with Prime ScriptTM RT reagent kit (TakaRa, Japan) according to the instruction book. SYBR Green PCR mastermix (Takara, Japan) was used for quantitative RT-PCR, and 10 μl reaction mixture was added into Axygen 384-well reaction plates sealed with optical adhesive covers (Axygen). The cDNA levels for *p53*, *Apaf1*, *Caspase3* and *Caspase7* were normalized to β -actin. The primers used for realtime PCR analysis were listed in Table 1 and Table 2. The ABI PRISM 7900HT instrument (Applied Biosystems, USA) was applied for quantitative RT-PCR with each sample prepared in triplicates. The program for quantitative PCR was run as follows: 95°C for 30 s, then 40 cycles were performed (5 s at 95°C and 31 s at 60°C), and then 95°C for 15 s, 60°C for 1 min, 95°C for 15 s.

TUNEL Assay

The testes of stress-treated newts and normal newts were dissected, and then wrapped in OCT compound (SAKURA, Japan) for section preparations with Micron HM525. TUNEL staining was performed on tissue sections using *in situ* cell death detection kit according to the instruction book (Beyotime, China). Briefly, the testis sections were firstly fixed using 4% paraformaldehyde (PFA) for one hour, and later washed three times with PBS. Then the sections were submerged in PBS with 0.1% Triton-X-100 in ice bath for 2 min. After further washes with PBS, the reaction was performed in the terminal deoxynucleotidyl transferase (TdT) buffer with fluorescein labeled dUTP, and the sample were incubated with reagent for one hour at 37°C with plastic membrane mounted to avoid reagent evaporation. Washed with PBS, the sections were incubated with mixture of DAPI and antifade reagent before coverglass mounting. The positive control was prepared by Positive TUNEL preparation kit (Beyotime, China), in which the sections were treated with DNase I for 30 min at 25°C and PBS wash before TUNEL labeling reaction. The TUNEL results were analyzed with a Zeiss laser scanning confocal microscope (LSM-710) (Carl Zeiss, USA).

Caspase Activity Assay

Caspase activities in testes of newts were analyzed using caspase activity assay kits, which were based on the capabilities of caspase-3, -8, -9 to cleave acetyl-Asp-Glu-Val-Asp p-nitroanilide (Ac-DEVD-pNA), acetyl-Ile-Glu-Thr-Asp p-nitroanilide (Ac-IETD-pNA) and acetyl-Leu-Glu-His-Asp p-nitroanilide (Ac-LEHD-pNA) respectively producing yellow formazan product p-nitroaniline (pNA). After heat shock (40°C , 2 h), cold exposure (4°C , 12 h), cadmium exposure (36 h) and starvation (one month), newts testes were dissected and rinsed with cold PBS, and then homogenized in ice bath using lysis buffer, with 5 min further extraction in ice bath. The tissue lysates were centrifuged at $18,000 \times g$ for 10 min at 4°C . Caspase-3, -8, -9 activities in the supernatant was assayed using the kit (Beyotime, China), and the absorbance at 405 nm was determined to quantify the caspase activities. All the experiments were performed in triplicates, and the caspase activities in the testes of stress-treated newts were presented as percentage of enzyme activity to that in control newts.

Transmission Electronic Microscopy (TEM)

The newt testis was initially fixed with 2.5% glutaraldehyde and then post-fixed in 1% osmium tetroxide solution at room temperature. After pre-stained with uranyl acetate, the sample was dehydrated with acetone and ethanol before their bedding in Spurr's resin. The sections were prepared with a Leica Ultracut UC6 Ultramicrotome (Leica Microsystems AG, Wetzlar, Germany). After staining with uranyl acetate and lead citrate, the sections were observed under transmission electronic microscopy (PHILIPS TECNAI 10).

Statistical Analysis

All data obtained in real-time RT-PCR and caspase activity assay were analyzed using EXCEL and SPSS 9.0 software and presented as mean \pm standard error. Student's T-test was used to evaluate the significant difference of gene expression levels and caspase activities between experimental group and control group. It was considered to be statistically significant when P value < 0.05 .

Results

The cDNA Sequences of p53, Apaf1, Caspase3 and Caspase7

We cloned the full-length cDNA of *p53*, *Apaf1*, *Caspase3* and *Caspase7*. *p53* (HM627863) has a full length of 1588 bp, including a 1179 bp open reading frame (ORF) encoding a putative protein of 392 amino acids (Aa) with the molecular weight of 44 KDa. The *Apaf1* (JQ320086) has a full length of 4313 bp, including a 3747 bp ORF encoding a putative protein of 1248Aa with a molecular weight of 140 KDa. The *Caspase3* (JQ320088) has a full length of 1218 bp with an 888 bp ORF encoding a putative protein of 295Aa with a molecular weight of 33 KDa. The *Caspase7* (JQ320087) has a full length of 2280 bp with an 897 bp ORF encoding a putative protein of 269Aa with a molecular weight of 34 KDa.

Protein Characterization of p53, Apaf1, Caspase3 and Caspase7

Apaf1 and p53. Multiple protein alignment of Apaf1 in *Cynops orientalis* with its homolog demonstrated that it owned 61.4% identity with its homolog in *Homo sapiens*, 55.7% in *Xenopus laevis*, 51.2% in *Danio rerio*, and 59.9% in *Mus musculus* (Figure 1). Protein structure prediction of Apaf1 showed Apaf1 consisted of

Figure 1. Multiple alignment of Apaf1 in *Cynops orientalis* with its homolog from several vertebrates. The protein alignment was created using Vector NTI10 (Invitrogen) with the following sequences: *Cynops orientalis*(JQ320086); *Homo sapiens* (O14727.2); *Mus musculus*(NP_033814.2); *Xenopus laevis*;(NP_001085834.1); *Danio rerio*(NP_571683.1). The identities of Apaf1 in *Cynops orientalis* with its homolog were 61.4% (*Homo sapiens*), 55.7% (*Xenopus laevis*), 51.2% (*Danio rerio*) and 59.9% (*Mus musculus*) respectively. doi:10.1371/journal.pone.0039920.g001

three functional subdomains: the N-terminal caspase recruitment domain (CARD) (1–89aa), the nucleotide-binding and oligomerization domain (NOD) (90–426) and the C-terminal WD40 domain. These functional subdomains of Apaf1 were indicated with arrows in its predicted 3-D structure (Figure 2).

Multiple protein alignment of p53 in *Cynops orientalis* with its homolog showed that it had 53.4% identity with its homolog in *Danio rerio*, 49.6% in *Homo sapiens*, 48.5% in *Mus musculus* and 52.8% in *Xenopus laevis*. Several amino acids (Ser235, Arg242, Arg267, Ala270, Cys271 and Arg274) that were essential for DNA binding are found conserved in this protein (Figure 3). The subdomains prediction showed p53 protein owned four functional domains: N-terminal transactivation domain (1–28Aa), proline-rich domain (58–101Aa), DNA binding domain (102–293Aa), tetramerization domain (315–357Aa) and C-terminal domain, which were indicated with arrows in predicted p53 3-D structure (Figure 4).

Caspase3 and caspase7. Multiple protein alignment of Caspase3 and Caspase7 in *Cynops orientalis* with their homolog showed that Caspase3 in *Cynops orientalis* have 56.2% identity with *Danio rerio* homolog, 54.4% with *Xenopus laevis*, 57.6% with *Homo sapiens* and 56.3% with *Mus musculus*. Caspase7 had 67.6% identity with *Danio rerio* homolog, 64.6% with *Xenopus laevis*, 62.6% with *Homo sapiens* and 62.3% with *Mus musculus*. His134 and Cys176 in Caspase3, and His149 and Cys191 in Caspase7 were predicted to be critical for catalytic activity and they were conserved compared with their homolog (Figure 5). The putative cleavage sites at Asp39 and Asp188 in Caspase3, and Asp24 and Asp30 in Caspase7 were also highly conserved, at which Caspase3 and Caspase7 can be separated into functional large subunit and small subunit respectively (Figure 5). The predicted subdomain structures of putative Caspase3 and Caspase7 in *Cynops orientalis* were very similar. They shared 50.6% identity, and both of them had conserved Asp cleavage sites and four loops that contributed to catalytic groove conformation. Additionally, the predicted 3-D

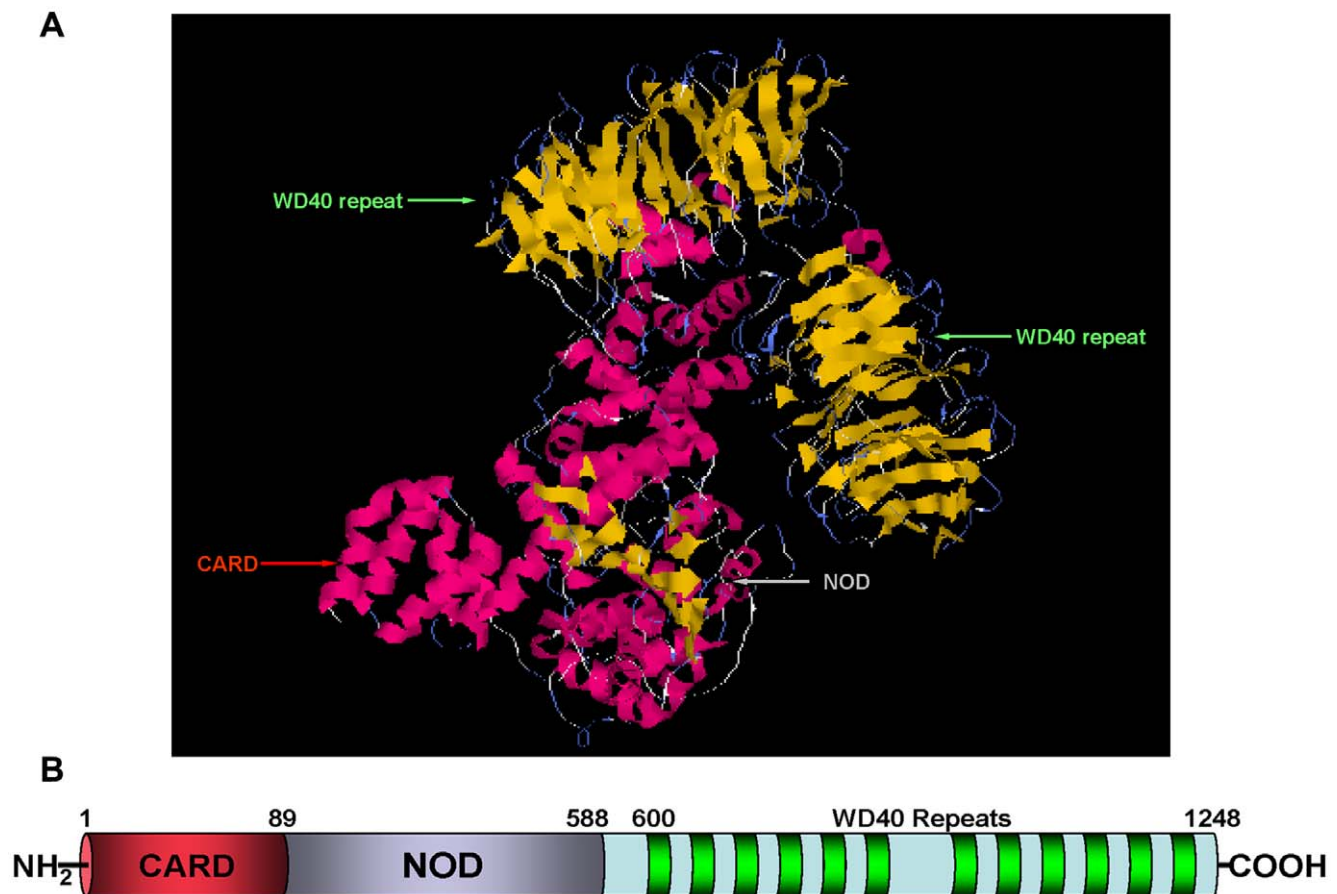


Figure 2. Predicted protein structure of Apaf1 in *Cynops orientalis*. (A) Cartoon representation of Apaf1 3-D structure. Yellow color stands for β -sheet and red color indicates the α -helix. The functional domains in the 3-D structures are indicated with arrows. The 3-D structure prediction was performed by I-TASSER server. (B) Schematic representation of Apaf1 subdomain structure. The subdomains are shown by the horizontal bar, with the numbers corresponding to the amino acid residues. The putative Apaf1 protein consists of three functional subdomains: the N-terminal caspase recruitment domain (CARD); the nucleotide-binding and oligomerization domain (NOD) and the C-terminal WD40 domain. doi:10.1371/journal.pone.0039920.g002

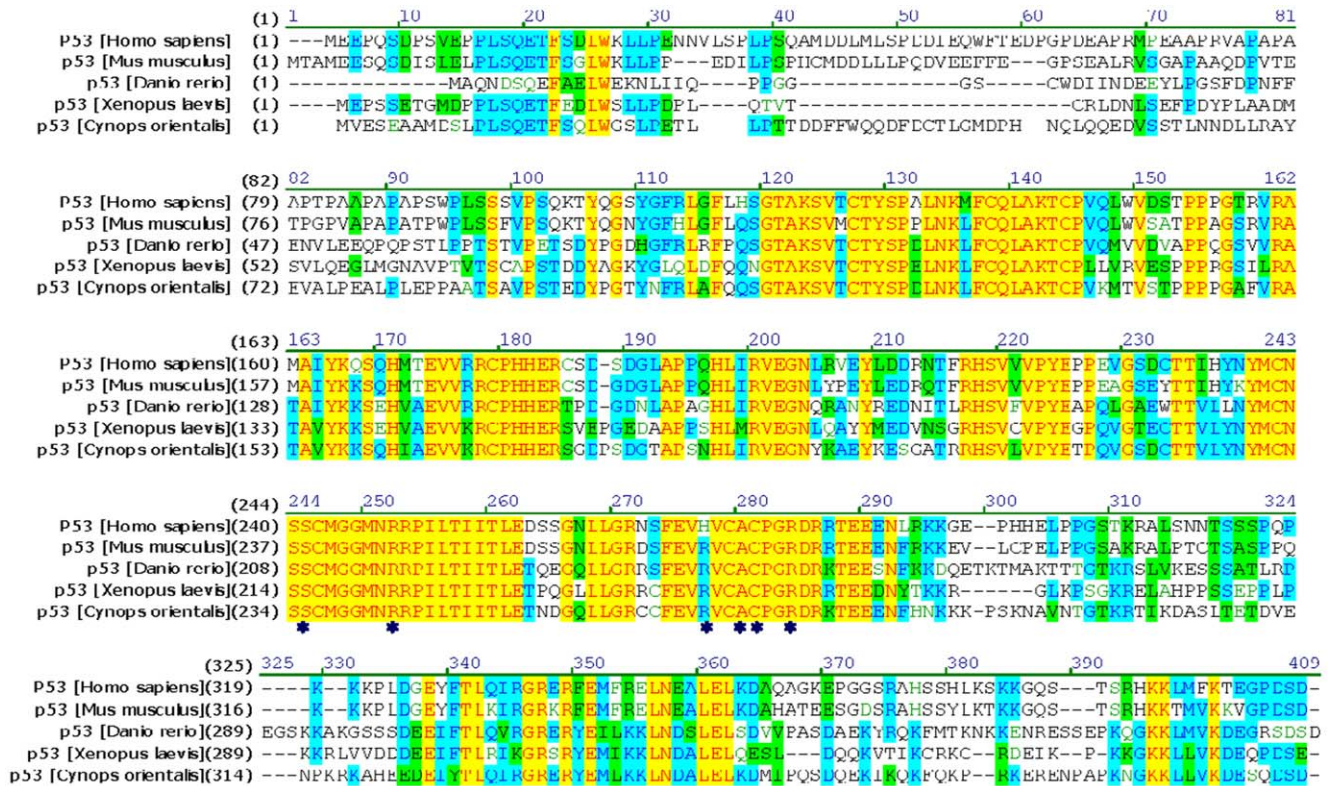


Figure 3. Multiple alignment of p53 in *Cynops orientalis* with its homolog from several vertebrates. The protein alignment was performed using Vector NTI10 (Invitrogen) with the following sequences: *Cynops orientalis* (HM627863)/*Homo sapiens* (BAC16799.1); *Mus musculus* (BA82343.1); *Xenopus laevis* (CAA54672.1); *Danio rerio* (NP_571402.1). The identities of p53 in *Cynops orientalis* with its homolog were 53.4% (*Danio rerio*), 49.6% (*Homo sapiens*), 48.5% (*Mus musculus*) and 52.8% (*Xenopus laevis*) respectively. Several amino acids that are essential for DNA binding are labeled with asterisks.

doi:10.1371/journal.pone.0039920.g003

structures of Caspase3 and Caspase7 also had high similarity (Figure 6).

Tissue specific Gene Expression of p53, Apaf1, Caspase3 and Caspase7

RT-PCR result showed that *p53*, *Apaf1*, *Caspase3* and *Caspase7* were expressed in various examined tissues. In the testis, *Caspase3* and *Apaf1* were expressed at slightly higher level than *p53* and *Caspase7* (Figure 7).

Gene Expression of p53, Apaf1, Caspase3 and Caspase7 in the Testis after Stress Treatment

In the testes of starved newts, gene expression of *p53* was slightly but significantly decreased while *Apaf1* didn't showed significant alteration. Notably *Caspase3* showed a more than 20-fold significant increase in its gene expression whereas *Caspase7* show no significant change (Figure 8 A and B). After cadmium exposure for 12 h, 24 h and 36 h, the expression of *p53* showed slight but significant decrease while *Apaf1* was slightly increased though without significance. Gene expression of *Caspase3* and *Caspase7* were decreased after cadmium exposure for 12 h and 24 h, but only the change of *Caspase3* mRNA level was significant. After 36 h exposure to cadmium, *Caspase3* gene expression was increased by about 8 fold though without significance, whereas no significant alteration of *Caspase7* was detected (Figure 8C and D).

After 4 h exposure to cold, gene expression of *p53* in newt testis was significantly decreased whereas its expression was elevated after 12 h though without significance. Differently the gene expression of *Apaf1* were decreased but only showed significant difference after cold exposure for 12 h. Gene expression level of *Caspase3* was greatly increased after cold exposure though without statistical significance whereas *Caspase7* didn't showed significant change after cold exposure (Figure 9A and B). In heat shock group, expression of *p53* showed significant decrease after exposure to 40°C, and no significant change was found after exposure to 38°C. *Apaf1* was only significantly increased after exposure to 38°C for 2 h, without any significant changes in other groups. *Caspase3* were significantly increased after heat shock at 40°C for 2 h and 38°C for 24 h without no significant alterations in other groups. *Caspase7* was only significantly increased in the testes of newts exposed to 38°C for 24 h (Figure 9C and D).

TUNEL Analysis of Germ Cell Apoptosis in Newt Testis

TUNEL assay showed spontaneous germ cell apoptosis occurred in the testis of normal newts, and apoptotic early spermatids (Figure 10A1-3) and mature sperms (Figure 11A1-3) were detected. Compared with normal newts, TUNEL results showed severer germ cell apoptosis occurred to early spermatids and mature sperm in the testis of newts treated by starvation (Figure 10B1-3, Figure 11B1-3), cold exposure (4°C for 12 h) (Figure 10 C1-3, Figure 11 C1-3), cadmium exposure (36 h) (Figure 10 D1-3, Figure 11 D1-3) and heat shock (40°C for 2 h)

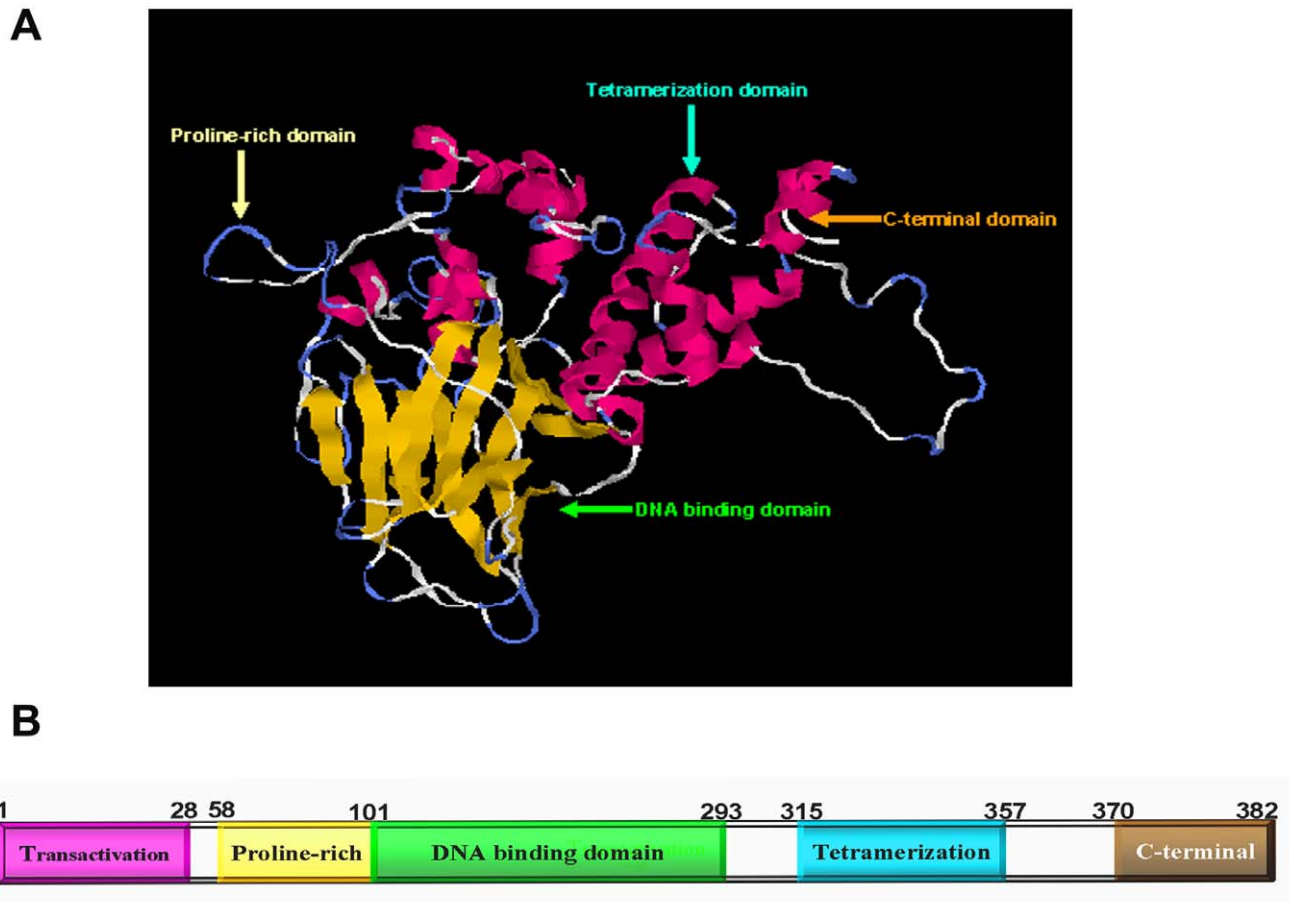


Figure 4. Predicted protein structure of p53 in *Cynops orientalis*. (A) Cartoon representation of p53 3-D structure. Yellow color stands for β -sheet and red color indicates the α -helix. The functional domains in the 3-D structure are indicated with arrows. The 3-D structure prediction was performed by I-TASSER server. (B) Schematic representation of p53 subdomain structure. The subdomains are shown by the horizontal bar, with the numbers corresponding to the amino acid residue. Several functional domains are in the p53: the transactivation domain, proline-rich domain, DNA binding domain, tetramerization domain and the C-terminal domain.
doi:10.1371/journal.pone.0039920.g004

(Figure 10 E1-3, Figure 11 E1-3). But no apoptotic spermatogonia were observed in the testes of normal newts and stress-treated newts (Figure 12 A and B). In positive TUNEL control sections, strong spermatogonia apoptosis was detected (Figure 12 C).

Caspase Activity Alteration in Newt Testes after Stress Treatment

In response to starvation, Caspase3 and Caspase8 activities in newt testes were increased to 166% and 112% while Caspase9 activity was decreased to 65% of the control. Under cadmium exposure, Caspase-3, -8, -9 activities were significantly elevated to 202%, 194% and 180% of the control. The activities of Caspase3, Caspase8 and Caspase9 were significantly increased to 182%, 245% and 149% after cold exposure (4°C 12 h), and elevated to 238%, 239% and 196% after heat shock (40°C 2 h) (Figure 13).

Ultrastructure of Newt Mature Sperm

The TEM results showed that the nucleus of newt mature sperm was long and narrow shaped (Figure 14 A). A large number of mitochondria were observed arranged surrounding the sperm nucleus (Figure 14 B).

Discussion

p53, Apaf1, Caspase3 and Caspase7 were Conserved in Chinese Fire-belly Newt, *Cynops Orientalis*

We have cloned the full-length cDNA of *p53*, *Apaf1*, *Caspase3* and *Caspase7* from the testis of Chinese fire-belly newt, *Cynops orientalis*. p53 and Apaf1 protein share about 50% identity with their homolog, and they have conserved functional subdomains. The DNA binding domain of p53 is highly conserved and six key amino acids essential for binding capability are totally the same among the examined homolog [58]. Besides, the transactivation domain and proline-rich domain conferred p53 possible capability in gene expression regulation while tetramerization domain indicated p53 probably became functional in a tetramer form [58,59]. As for Apaf1, CARD is an essential functional domain because it is responsible for recruiting procaspase9 for apoptosome formation [24,25,60]. The NOD domain is involved in Apaf1 oligmerization into apoptosome [61], and the C-terminal 12 WD40 repeats contributed to cytC binding to initiate downstream cascade of caspases [24,25,61,62,63]. The 3-D structure of p53 and Apaf1 was quite similar to their counterparts in mammals [58,64]. Base on the highly conserved subdomain structures and

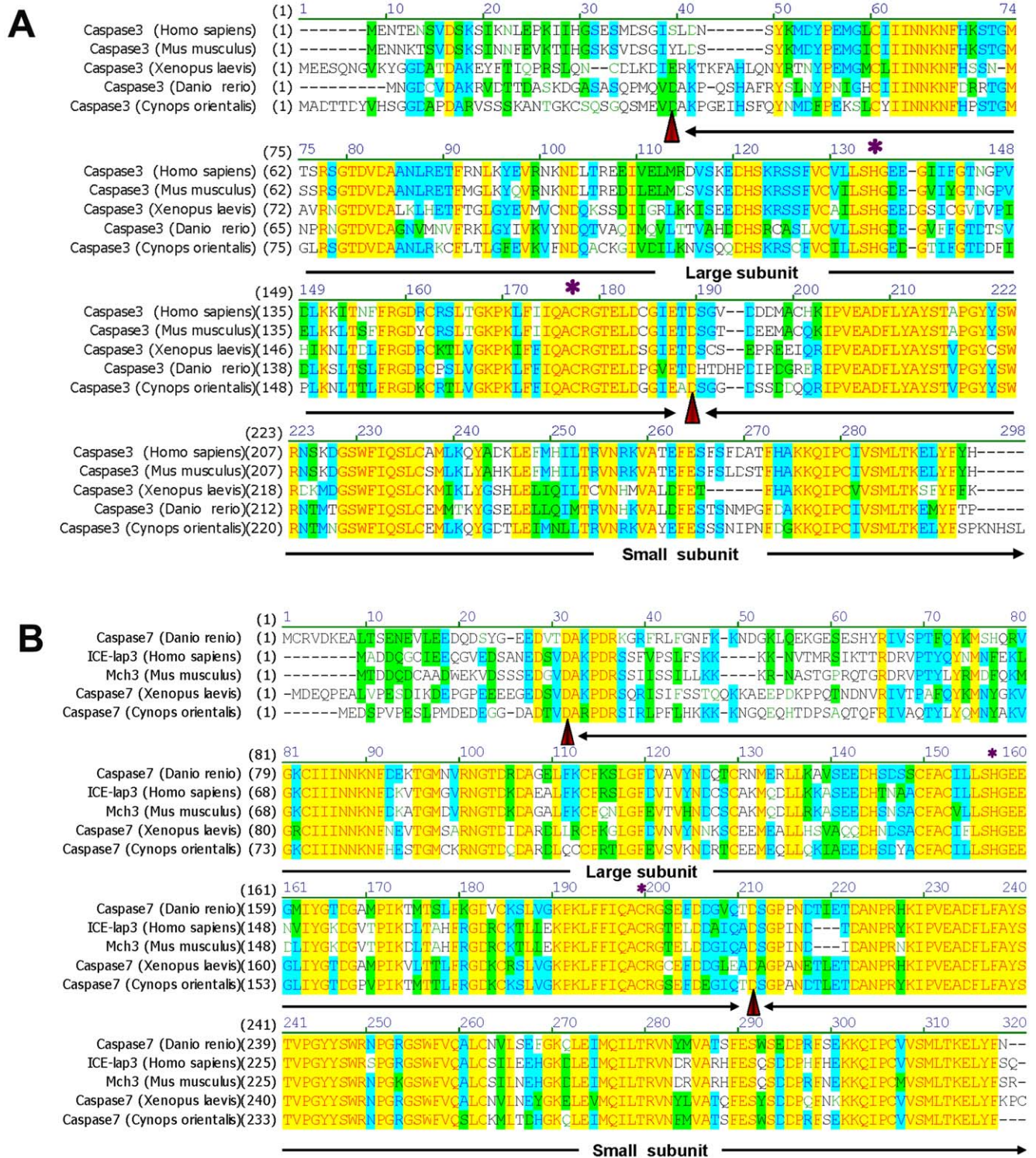


Figure 5. Multiple alignments of Caspase3 and Caspase7 in *Cynops orientalis* with their homolog from several vertebrates. The protein alignment was performed using Vector NT110 (Invitrogen) with the following sequences: (A) *Cynops orientalis*(JQ320088); *Danio rerio*(CAX14649.1); *Xenopus laevis* (NP_001081225.1); *Homo sapiens* (P42574); *Mus musculus* (P70677); (B) *Cynops orientalis* (JQ320087); *Homo sapiens* (AAC50346.1); *Mus musculus*(BAA19730.1); *Xenopus laevis* (NP_001091272.1); *Danio rerio* (AAH95327.1). The identities of Caspase3 in *Cynops orientalis* with its homolog were 56.2% (*Danio rerio*), 54.4% (*Xenopus laevis*), 57.6%(*Homo sapiens*) and 56.3% (*Mus musculus*). The identities of Caspase7 in *Cynops orientalis* with its homolog were 67.6% (*Danio rerio*), 64.6% (*Xenopus laevis*), 62.6% (*Homo sapiens*) and 62.3% (*Mus musculus*). Putative cleavage sites at aspartic acid residues, which separate Caspase3 and Caspase7 into large subunits and small subunits, are labeled red arrowheads. Histines and Cystines that are essential for the catalytic centre of Caspase3 and Caspase7 are indicated by asterisk.

doi:10.1371/journal.pone.0039920.g005

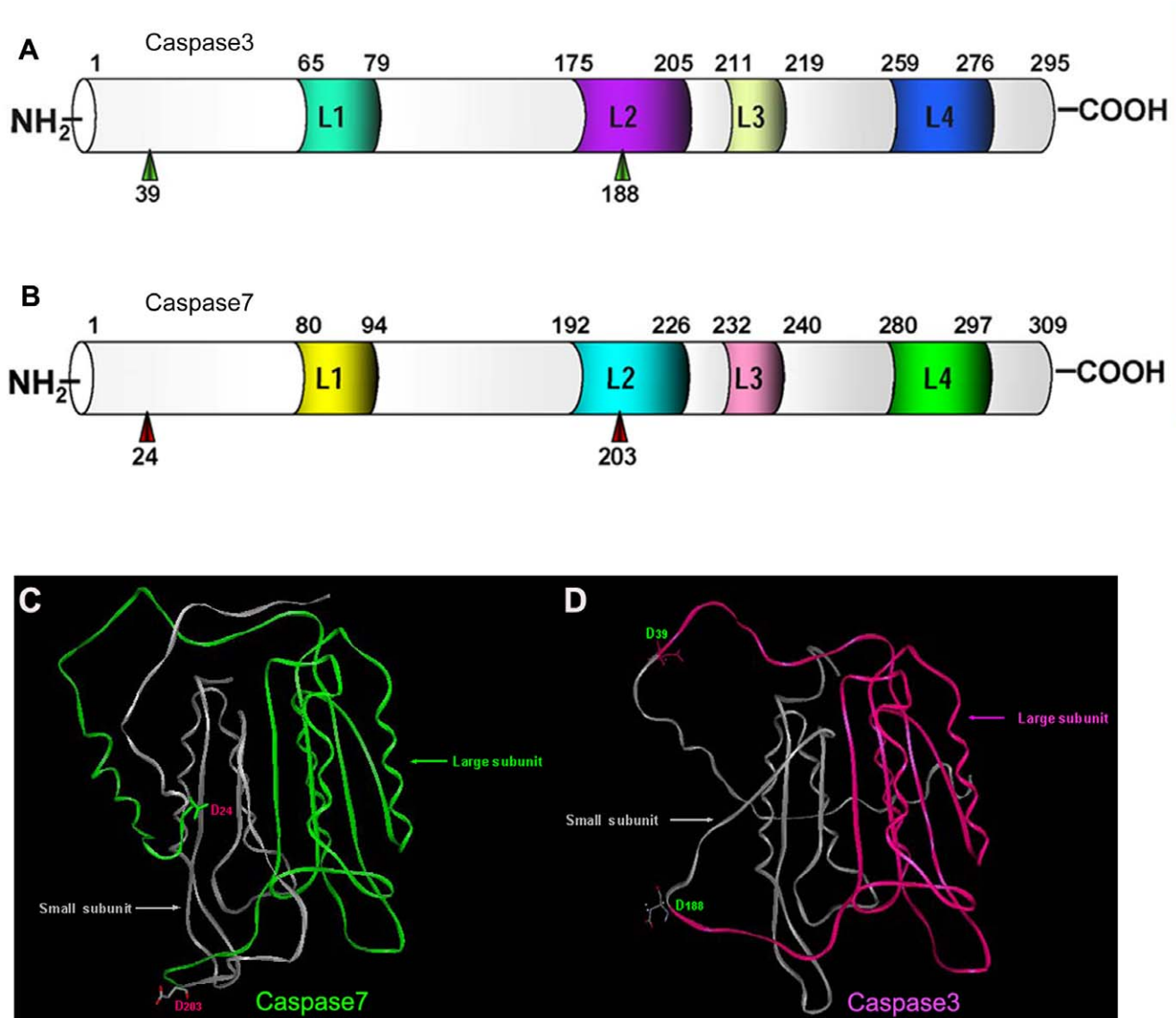


Figure 6. Predicted protein structures of Caspase3 and Caspase7 in *Cynops orientalis*. (A)(B) Schematic representation of the predicted subdomain structure of Caspase3 (A) and Caspase7 (B) in *Cynops orientalis*. The subdomains are shown by the horizontal bar, with the numbers corresponding to the amino acid residues. The cleavage active Aspartine are marked with green or red arrow head, which separate the Caspase3 or Caspase7 into large subunits and small subunits. The four surface loops (L1-L4) that shape the catalytic groove are also labeled with different colors. (C)(D) Cartoon representation of the 3-D structures of Caspase3 and Caspase7. The red color and green stands for the large subunit of Caspase3 and Caspase7, and the gray color indicates the small subunits of Caspase7 and Caspase3. Two cleavage active Asp residues are shown with the form of stick and ball in the cartoon. The 3-D structure prediction was performed by I-TASSER server.
 doi:10.1371/journal.pone.0039920.g006

similar 3-D structures, p53 and Apaf1 in newts probably performed similar functions to their homolog in mammals.

Caspase3 and Caspase7 showed 54%–57% and 62%–67% identity with their homolog respectively. As critical cleavage sites, Asp24/Asp203 (Caspase7) and Asp39/Asp188 (Caspase3) are conserved, revealing a similar cleavage mechanism. Besides, being key catalytic residues, the highly conserved His134/Cys176 (Caspase3) and His149/Cys191 (Caspase7) indicated an similar catalytic performance [65,66]. As effector caspases, Caspase3 and Caspase7 in *Cynops orientalis* have highly similar subdomain structure and 3D structures, which further demonstrated that their similar performance in cell apoptosis resulted from resembled structures [67].

RT-PCR results showed that *p53*, *Apaf1*, *Caspase3* and *Caspase7* were expressed in various examined tissues. In the testis, *Caspase3* and *Apaf1* were expressed at higher level than *p53* and *Caspase7*, which indicated more active *Caspase3* and *Apaf1* in newt testis. *Caspase3* and *Caspase7* have been found expressed during normal spermatogenesis, and play important functions in spontaneous germ cell apoptosis [23]. *p53* and *Apaf1* were also proved expressed in testis, and they are critical for sperm development and male fertility [23,68,69]. Knockout or overexpression of *p53* would result in abnormal spermatogenesis [22,23] while knockout of *Apaf1* could induce male infertility [70].

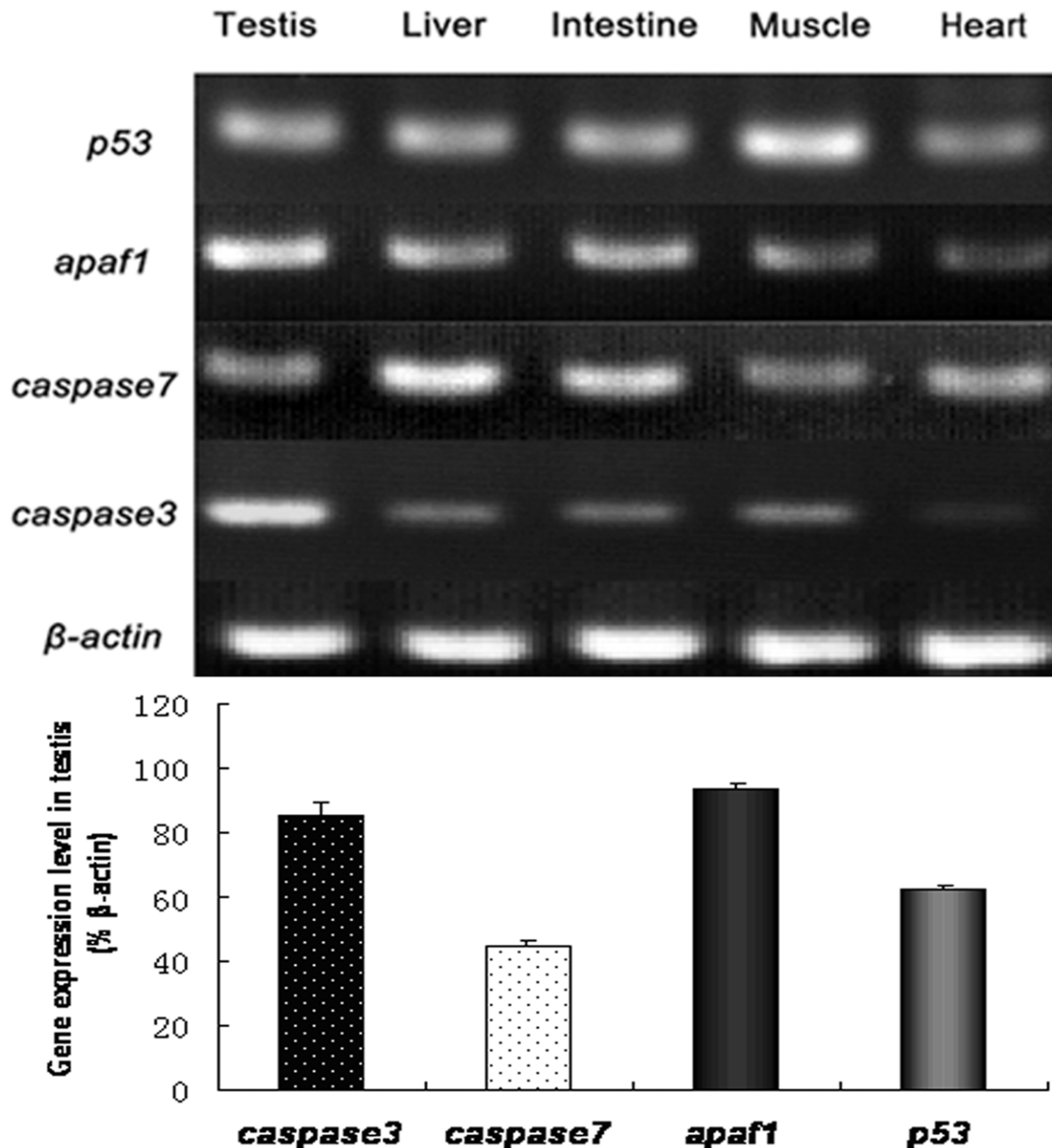


Figure 7. *p53*, *apaf1*, *caspase3* and *caspase7* gene expression in various tissues of *Cynops orientalis*. Total RNA was extracted from fresh testis, muscle, liver, intestine and heart, and then transcribed into cDNA for RT-PCR analysis. β -actin served as an internal control. *p53*, *apaf1*, *caspase3* and *caspase7* are expressed in all the examined tissues. In the newt testis, *Apaf1* and *Caspase3* were expressed at higher level than *p53* and *Caspase7*. The intensity of the signal was analyzed by Tanon-Gis system and the data were processed with SPSS 9.0. The gene expression level in testis were presented as their percentage of β -actin. Significance of difference was assessed by SPSS9.0. $P < 0.05$. $n = 3$. doi:10.1371/journal.pone.0039920.g007

Spontaneous Germ Cell Apoptosis Occurred in Newt Testis

During normal spermatogenesis, spontaneous germ cell apoptosis commonly occurred to spermatogonia and spermatocytes in many mammalian species including rats, hamsters, mice and humans [2,3,4,5,6,7,8,9,45,71,72,]. Since the spermatogonia and spermatocytes were active in DNA replication, which made them vulnerable to damage [21,45,73,74,75]. In some cases, apoptosis even occurred to spermatids or sperm, though the frequency is low [2,76]. In the present study, we only observed apoptotic

spermatids and sperm without apoptotic spermatogonia and spermatocytes detected, whereas severe apoptotic spermatogonia were observed in positive control sections. The result indicated the intriguing germ cell apoptosis in newts was probably resulted from specificity of this species. The spontaneous germ cell apoptosis in newt testis may be responsible for clearing off abnormal spermatogenic cells and ensuring production of high quality sperm [27,28,30,77].

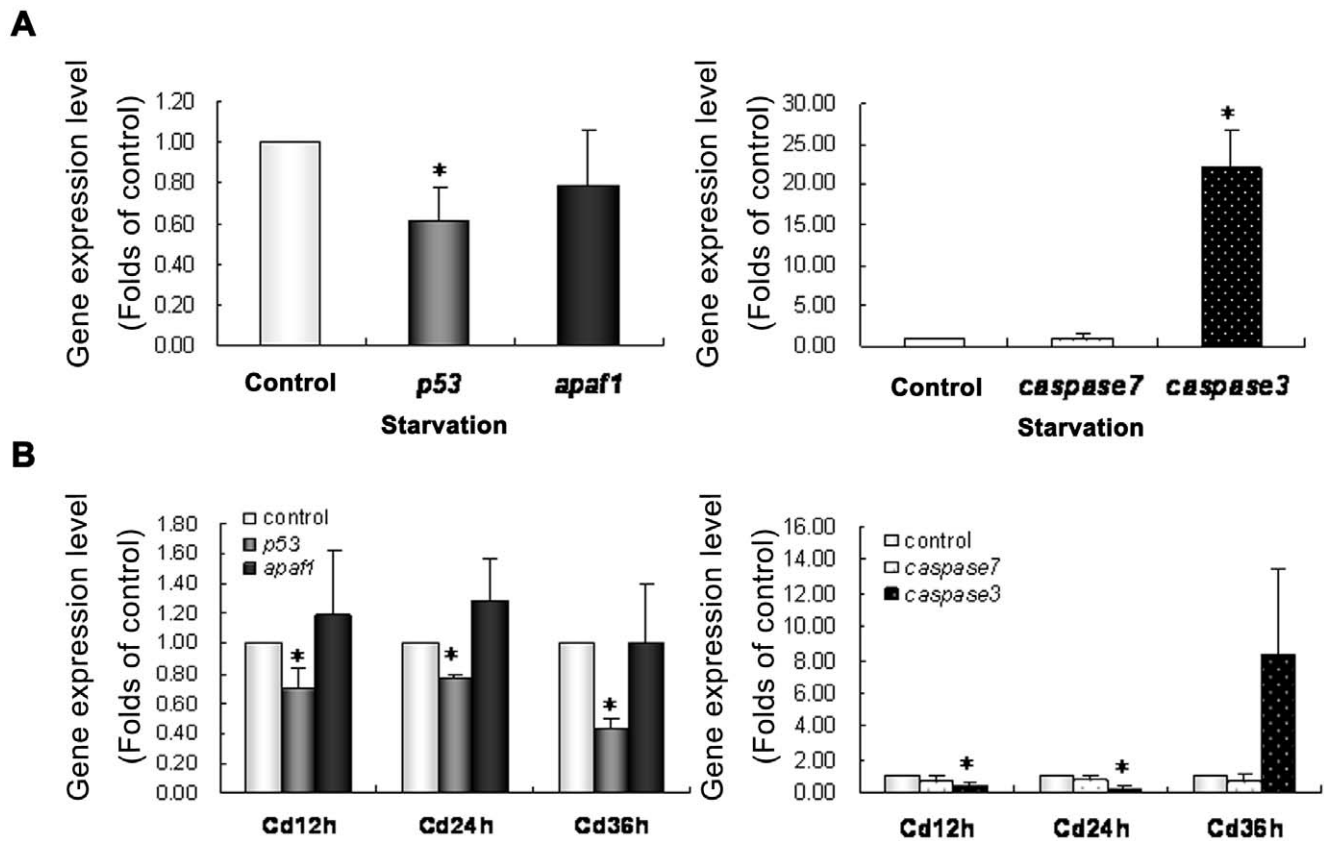


Figure 8. *p53*, *Apaf1*, *Caspase3* and *Caspase7* gene expression in the testis of *Cynops orientalis* after starvation and cadmium exposure. (A)(B) gene expression level after starvation (one month). (C)(D) gene expression level after cadmium exposure determined by real-time reverse transcription-PCR. Messenger RNA levels in experimental group were presented as the folds of gene expression level in control group, which was set as 1.0. All data were expressed as Means \pm SD, and T-test in SPSS9.0 applied to analyze the significance of differences between experimental group and control group. * $P < 0.05$ when compared with control. $n = 3$. doi:10.1371/journal.pone.0039920.g008

Caspase3 and Caspase7 are Involved in Stress-induced Germ Cell Apoptosis

When spermatogenesis was threatened by environmental or physiological stress, stress-induced germ cell apoptosis was often initiated to remove abnormal germ cells [78,79,80]. For instance, hormone deprivation, heat shock, low temperature, starvation and heavy metal exposure could aggravate germ cell apoptosis in testes [50,77,81,82]. In our research, negative effects were exerted by cadmium exposure (36 h), heat shock (40°C 2h), cold exposure (4°C 12h) and starvation (one month) on germ cell maturation in newt, leading to severer spermatid and sperm apoptosis. Obviously, the germ cell development in *Cynops orientalis* was vulnerable to stress, and germ cell apoptosis had been triggered by temperature stress, starvation and heavy metal exposure.

Caspase3, Caspase6 and Caspase7 were three important effector caspases that directly determined cell death in cell apoptosis signaling pathway [66,83]. Previous researches on newts have demonstrated that high caspase activity in toxicant-treated testes was responsible for chromatin condensation and apoptotic body formation [49]. In our study, after stress treatment, not only gene expressions of *Caspase3* or *Caspase7* in newt testis were obviously elevated, but also the Caspase3 enzyme activity in the testis was significantly increased. Therefore, the stress-induced germ cell apoptosis was dependent on both gene expression and enzyme activation of Caspase3.

Possible Mechanism for Starvation-induced Germ Cell Apoptosis

Nutrients are essential for male reproduction performance, for it can supply energy like glucose and growth factors that tightly correlates with cell metabolism, growth and proliferation [84,85]. Without sufficient growth factor and glucose, cells firstly reduced its metabolism and ceased proliferation, and further nutrients deprivation would initiate cell apoptosis [86,87,88,89,90,91,92,93]. In our study, after one-month food deprivation, we found severer germ cell apoptosis occurred in the testis of *Cynops orientalis* compared with control newt, which probably resulted from serious shortage of growth factor and glucose. It was demonstrated that cell apoptosis triggered by nutrients deprivation was caspase-dependent, and executed mainly by intrinsic mitochondria-dependent pathway [85,94,95,96]. In detail, nutrients deprivation could change cellular metabolism, and disrupted the overall balance between proapoptotic and anti-apoptotic Bcl-2 family members. Then mitochondrial physiology would be altered to facilitate cytC release into the cytosol. Together with Apaf1 and procaspase9, cytC was assembled into the apoptosome to activate caspase9 that further activated effector caspases to induce cell death [93,97,98]. In addition, p53 was elucidated to be involved in starvation-induced cell apoptosis [99], and Fas-dependent extrinsic pathway proved critical for germ cell apoptosis after growth factor withdrawal [100]. However, in our study, after one month starvation, either the gene expression of

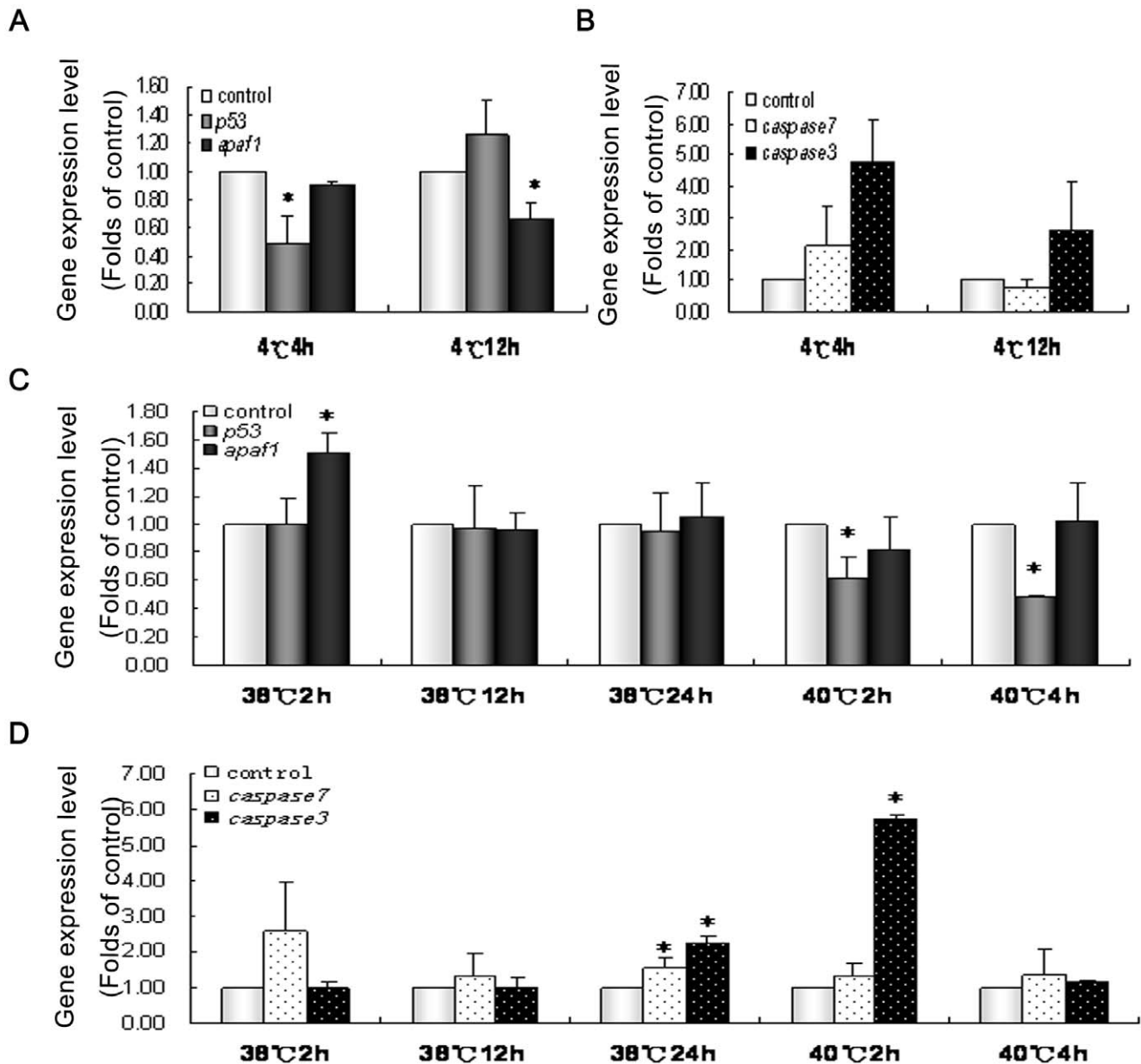


Figure 9. *p53*, *Apaf1*, *Caspase3* and *Caspase7* gene expression after stress treatment. The gene express pattern in the testis of *Cynops orientalis* after cold exposure at (4°C 4 h and 12 h) and heat exposure (38°C 2 h, 12 h and 24 h; 40°C 2 h and 4 h) determined by real-time reverse transcription-PCR. Messenger RNA levels in experimental group were presented as the folds of gene expression level in control group, which was set as 1.0. All data were expressed as Means \pm SD, and T-test in SPSS9.0 applied to analyze the significance of differences between experimental group and control group. * P<0.05 when compared with control. n = 3. doi:10.1371/journal.pone.0039920.g009

Apaf1 and *p53* or Caspase9 enzyme activity in the testis of *Cynops orientalis* was significantly decreased. Therefore intrinsic pathway was probably not involved in starvation-induced germ cell apoptosis. In contrast, Caspase8 enzyme activity in the testis was slightly elevated after starvation treatment, which indicated that the extrinsic pathway might participate in the starvation-induced germ cell apoptosis in *Cynops orientalis*.

Possible Mechanism for Cadmium-induced Germ Cell Apoptosis

Cadmium is one of the most toxicants in terrestrial and aquatic environment, and both cadmium pollution and cadmium

injection into testis can induce testicular impairment, germ cell death, poor semen quality and even male infertility [80,101,102,103,104,105,106,107]. Cadmium triggered germ cell apoptosis by disrupting endocrine secretion and enhancing reactive oxygen species (ROS) production. On the one hand, cadmium is an endocrine disruptor that can affect functions of Leydig cell and inhibit testicular testosterone secretion [4,35,108,109,110,111,112,113], both of which were essential for spermatogenesis [2,114,115]. Once the testosterone was inhibited by cadmium, massive testicular germ cell apoptosis would occur [101,106]. Fas and FasL have been elucidated to play pivotal roles in germ cell apoptosis after testosterone

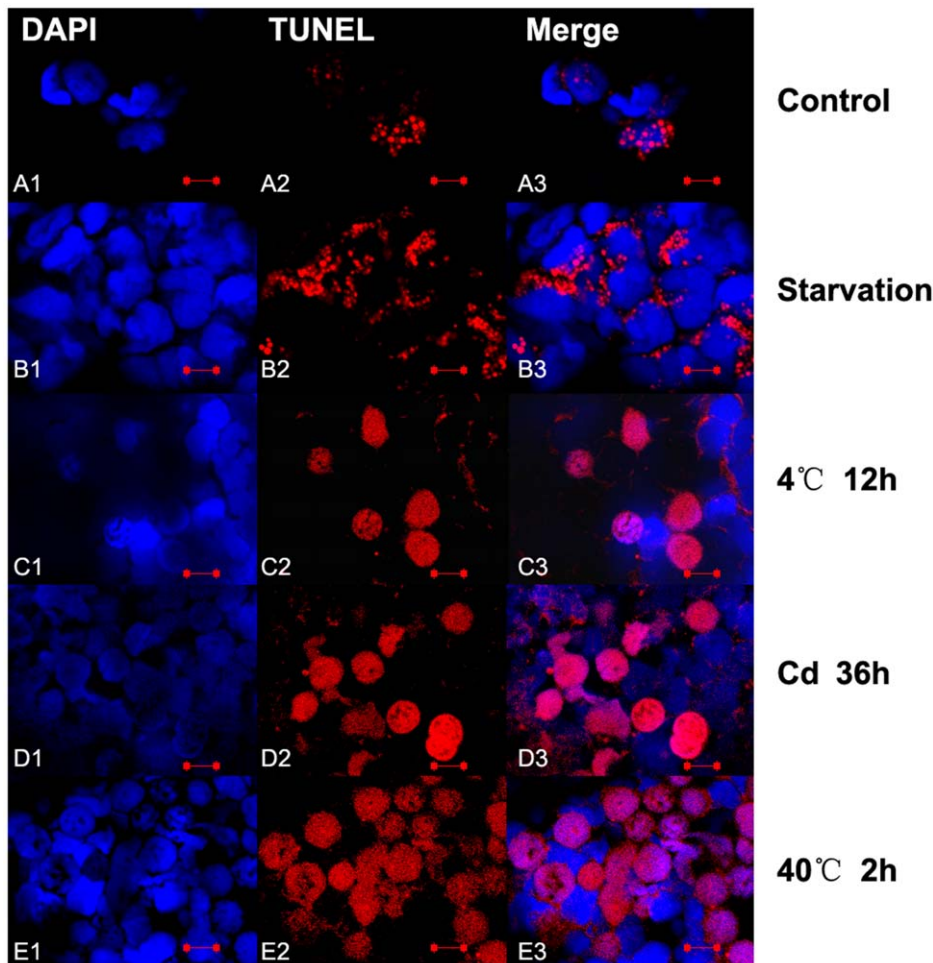


Figure 10. Immunofluorescence analysis of spontaneous apoptosis and stress induced apoptosis in newt early spermatids. The apoptotic germ cells were determined by TUNEL kit (red signal) (Beyotime, China) and the nucleus were dyed with DAPI (Blue signal). Apoptotic sperms were found in normal newt testis (A1-3), and severer mature sperm apoptosis detected under various stress including starvation (B1-3), cold exposure (4°C for 12 h) (C1-3), cadmium exposure (5 mg/Kg body weight for 36 h) (D1-3) and heat exposure (40°C for 2 h) (E1-3). The scale bar is 10 μ m.

doi:10.1371/journal.pone.0039920.g010

deprivation and cadmium exposure, with their gene expression increased both in germ cells and Sertoli cells [32,35,36,77,80,103,116,117]. In this study, the enzyme activity of Caspase8 in the testis was elevated by 100%, and it demonstrated that the cadmium exposure probably disrupted the hormone secretion and the extrinsic cell death pathway was initiated. On the other hand, cadmium could induce germ cell apoptosis by enhancing generation of ROS like superoxide ion, hydroxyl radicals and hydrogen peroxide, and these oxidative stress could result in peroxidation, mitochondrial dysfunction or DNA damage in germ cell and oxidative damage in Leydig cells [80,118,119,120,121,122,123,124]. Oxidative stress could induce p53 mediated cell apoptosis in the intrinsic mitochondria-dependent pathway [125,126,127,128]. The Caspase9 enzyme activity in the testis was raised by 80%, and probably the mitochondria-dependent intrinsic pathway was also involved in the cadmium-induced germ cell apoptosis. As the key participant of intrinsic cell death pathway, Apaf1 probably participate in the cell apoptosis in spite of no elevation in its gene expression.

Under oxidative stress, p53 could be activated to promote reduced glutathione generation and sestrins expression, thus protecting DNA from damage by decreasing ROS [129]. But we

found that gene expression of *p53* was reduced after cadmium exposure, and previous study also showed cadmium suppressed *p53* gene expression in the testes and liver [101,130]. So we deduced that ROS induced by cadmium may result in devastating DNA damage, which directly lead to cell apoptosis in a p53-independent pathway.

Possible Mechanism for Heat- and Cold-induced Germ Cell Apoptosis

Suitable environmental temperature is important for male reproduction. Heat shock can induce germ cell death and even male infertility while cold temperature leads to abnormal sperm production [53]. In adult rat testis, heat shock (43°C for 15 min) caused germinal epithelium damage, abnormal Sertoli cell and germ cell death [11,131,132] that mainly occurred to meiotic spermatocytes and early spermatids [11]. The intrinsic mitochondria-dependent pathway proved critical for heat-induced germ cell apoptosis, in which Bcl-2 family members played important functions [77,81,133,134,135]. Bax induced the cyt C release from the mitochondria to initiate the activation of Caspase9, which eventually activated downstream effector caspases (caspase3, 6 and

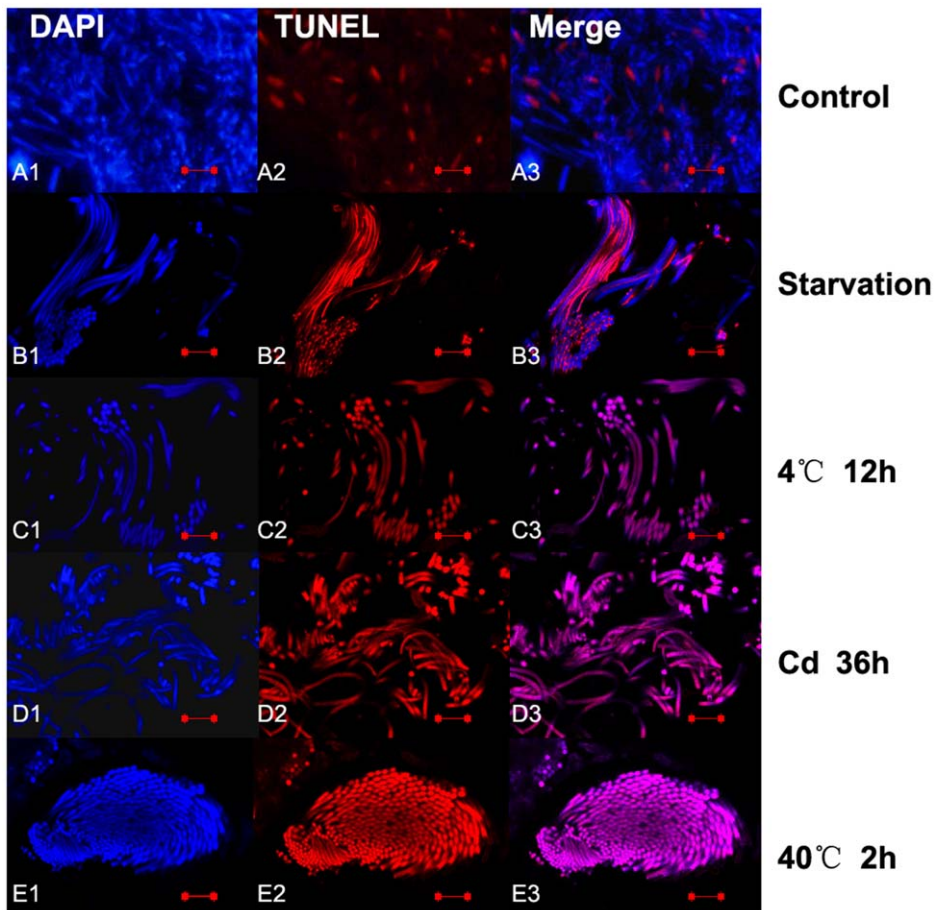


Figure 11. Immunofluorescence analysis of spontaneous apoptosis and stress induced apoptosis in newt mature sperms. The apoptotic germ cells were determined by TUNEL kit (Beyotime, China) and the nucleus were dyed with DAPI. Apoptotic sperms were found in normal newt testis (A1-3), and severer mature sperm apoptosis detected under various stress including starvation (B1-3), cold exposure (4°C for 12 h) (C1-3), cadmium exposure (5 mg/Kg body weight for 36 h) (D1-3) and heat exposure (40°C for 2 h) (E1-3). The scale bar is 10 μ m. doi:10.1371/journal.pone.0039920.g011

7) leading to cell death [81,136]. Moreover, Fas-dependent extrinsic pathway was also involved in heat-induced testicular germ cell apoptosis in cryptorchid testis [31]. We detected that enzyme activities of Caspase8 and Caspase9 in newt testis were significantly enhanced by 139% and 96% respectively after heat shock, indicating the involvement of extrinsic and intrinsic pathway in the germ cell apoptosis. Though without significant

alteration, Apaf1 also should be involved in heat-induced germ cell apoptosis regarding its key status in intrinsic pathway. Though p53-dependent apoptosis was reported to be responsible for the initial phase of germ cell loss in experimental cryptorchid testis [31], *p53* gene expression was significantly decreased in our study, indicating it probably didn't participate in this process.

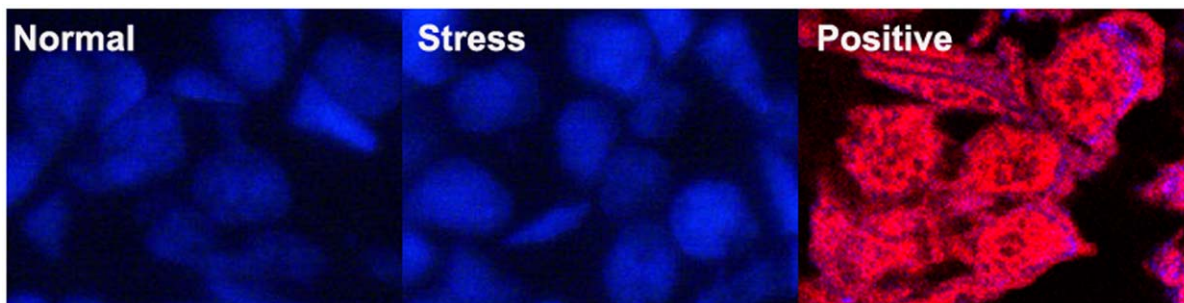


Figure 12. Immunofluorescence analysis on apoptosis. No apoptosis occurred to spermatogonia in normal newt testis and stress treated newt. The apoptotic germ cells were determined by TUNEL kit (red signal) (Beyotime, China) and the nucleus were dyed with DAPI (Blue signal). No apoptotic spermatogonia were found in normal newt testis (A) and stress treated newts (B) while severe apoptotic signal was in spermatogonia in the testis treated with DNase I in the TUNEL positive preparation Kit (Beyotime, China). The scale bar is 10 μ m. doi:10.1371/journal.pone.0039920.g012

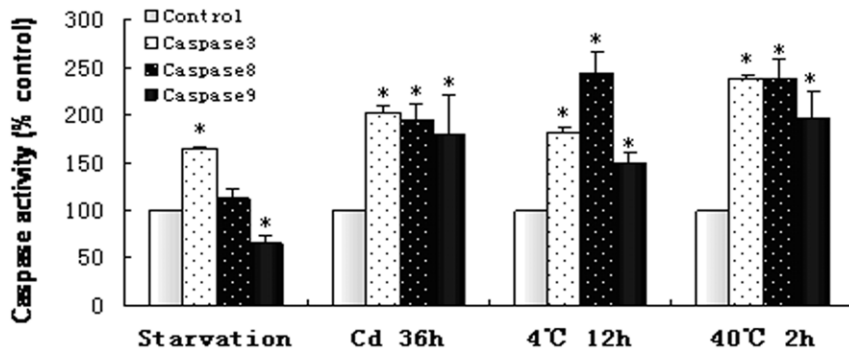


Figure 13. Caspase-3, -8, -9 activities in the testis of newts treated with various stress. The Caspase activities in the testis of newts were analyzed after stress treatment including starvation (one month), cadmium injection (36 h), cold exposure (4°C, 12 h) and heat exposure (40°C, 2 h). Caspase-3, -8, -9 activity was measured by colorimetric assays based on caspase-3, -8, -9 to change Ac-DEVD-pNA, Ac-IETD-pNA and Ac-LEHD-pNA into a yellow formazan product (pNA), respectively. The caspase activities in stress exposure groups were presented as the percentage of enzyme activity in the control group. Value represents the Mean±SD, and T-test in SPSS9.0 applied to analyze the significance of differences between stress treated group and control group. * P<0.05 when compared with control. n =3. doi:10.1371/journal.pone.0039920.g013

Low temperature could trigger germ cell apoptosis mainly by reducing FSH secretion, which was critical for male reproduction especially in seasonally breeding animals [53]. FSH not only supported proliferation and maturation of Sertoli cells [137], but also maintained spermatogonia viability and proliferation [52,138]. Additionally, FSH could inhibit PRL induced spermatogonia cell death both *in vivo* and *in vitro* [51,53]. In newts, spermatogonia apoptosis occurred after cold exposure for one week (12° and 8°C) whereas no degeneration was found in newts kept at 22°C. Notably, cold triggered germ cell death was significantly suppressed by FSH at 12°C and 22°C but not at 8°C [50,53], indicating the irremediable germ cell apoptosis induced by lower temperature. Therefore severe germ cell apoptosis triggered by cold exposure (4°C) in our research to a big extent

resulted from significant decrease in FSH secretion. It was elucidated that FSH can determine cell destiny by regulating several important proteins, including Survivin, PDCD6 and DR5, all of which were key members in intrinsic pathway and extrinsic pathway in cell apoptosis. High level of FSH could upregulate the expression of Survivin and suppress the expression of PDCD6 and DR5 [139], thus to promote cancer development and inhibit cell apoptosis. When FSH level in the testis was decreased after cold exposure, the expression of Survivin was probably reduced while the inhibition of PDCD6 and DR5 was terminated. In this way, both extrinsic and intrinsic pathway could participate in cold-induced germ cell apoptosis, which was evidenced by the significantly elevated enzyme activities of Caspase8 (150%) and Caspase9 (50%) in our research. Moreover increased gene

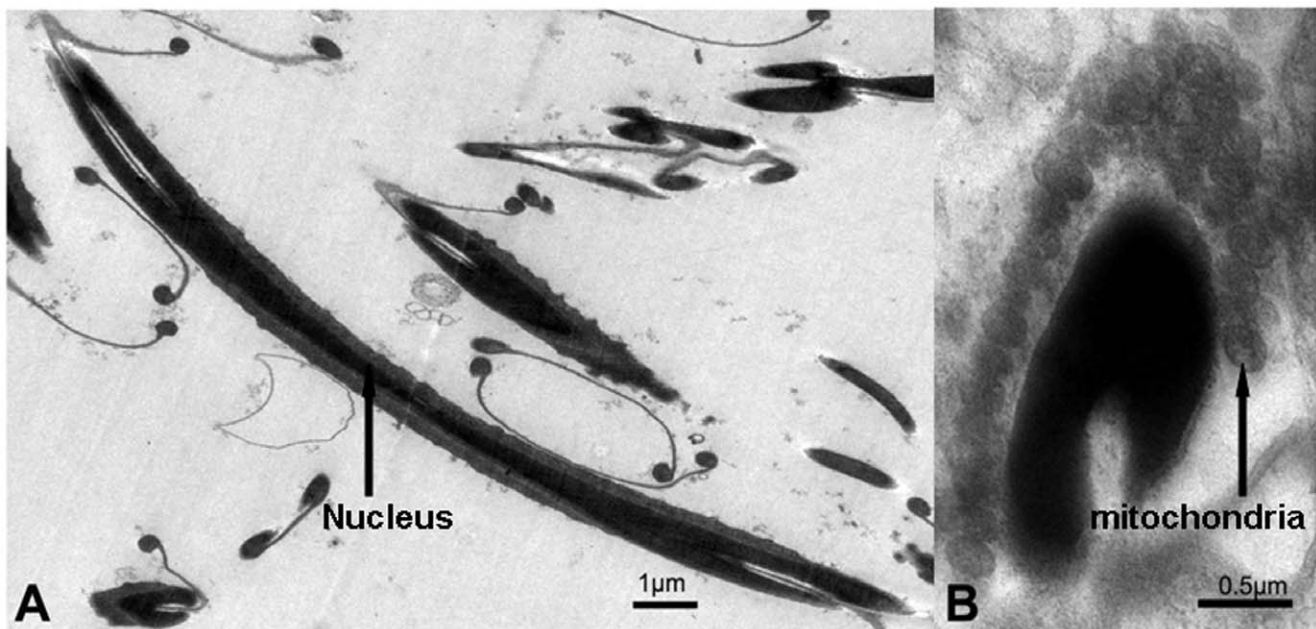


Figure 14. Ultrastructure of newt sperm. (A) Longitudinal section of the mature sperm. The nucleus is exceedingly long and thin (white arrow). Scale bar:1 µm (B) Cross section of the mature sperm nucleus. A large number of mitochondria were arranged around the nucleus (white arrow). Scale bar: 0.5 µm. doi:10.1371/journal.pone.0039920.g014

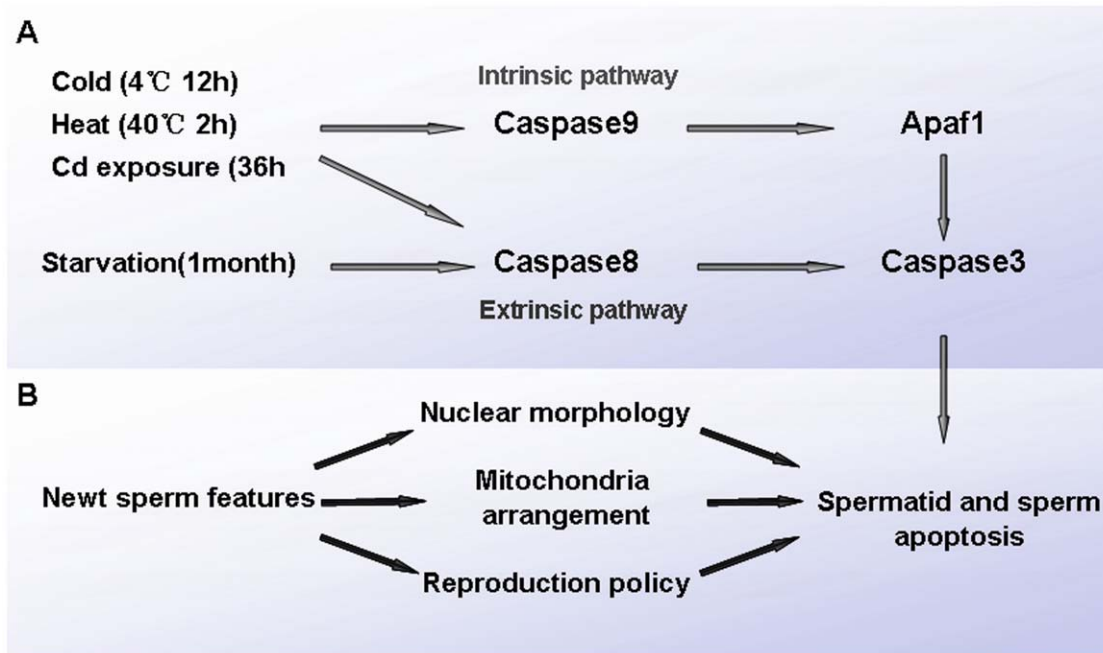


Figure 15. Schematic representation of possible mechanism for the stress triggered germ cell apoptosis in Chinese fire-belly newt, *Cynops orientalis*. (A) Potential pathways initiated by various stress in germ cell apoptosis. Cold exposure, cadmium exposure and heat exposure probably induced germ cell apoptosis via both extrinsic pathway and intrinsic pathway, but starvation likely only via extrinsic pathway. (B) Hypothesized sperm features and unique reproduction policy responsible for high occurrence of spermatid and sperm apoptosis. The nuclear morphology and mitochondria arrangement may be the physiological basis for observed high frequency of spermatid and sperm apoptosis, and a unique reproduction policy of newts may also account for this phenomenon.
doi:10.1371/journal.pone.0039920.g015

expression of Apaf1 indicated it probably participate in cell apoptosis while p53 may not for its decreased gene expression.

Possible Mechanism for Intriguing Sperm Apoptosis

The most intriguing phenomenon in our study is that germ cell apoptosis commonly occurred to spermatids and mature sperm, but not to spermatogonia and spermatocytes. Differently, other researches on newts only found apoptotic spermatogonia, spermatocytes and only abnormal mature sperm [47,48,49]. In previous researches, apoptotic mitotic diploid spermatogonia and meiotic primary spermatocytes were most common, and then was the apoptotic spermatids, either in spontaneous germ cell death or stress-induced cell apoptosis [3,45,140,141,142,143]. Only in recent years, more and more researches reported the occurrence of mature sperm apoptosis [76,144,145]. Several key apoptotic proteins were found in mature spermatozoa. For instance, in ejaculated mature sperm, functional p53 was localized in 43% of semen samples, and PARP in 75–100% of the sperm [144,146]. Moreover, active caspase1, caspase3 and caspase8 were found predominantly in the postacrosomal region of live sperm, and active caspase9 was particularly localized in the midpiece [76]. In human sperm, procaspases 8 and 9 and their active forms, together with caspase3, were also observed [146]. Furthermore, sperm fractions with low motility exhibit higher levels of active caspase3 compared with high-motility fractions [147]. Active caspase3 found in the sperm midpiece were closely associated with DNA fragmentation in low motility semen specimen, suggesting that caspase-dependent apoptotic mechanisms could originate in the cytoplasmic droplet or within mitochondria and function in the nucleus [148]. The activation of caspases in low-motility sperm samples may be attributed to the role played by cytC/Apaf-1

complex, which can activate caspase9 that was followed by activation of downstream caspase3, caspase6 and caspase7 [145].

We hypothesized that several physiological features of Chinese fire-belly newts might account for why mature sperm were easily involved in cell apoptosis. Above all, newt mature sperm had a long and narrow shaped nucleus which may be quite vulnerable to environmental stress (Figure 14 A). Moreover, similar to the mitochondria in midpiece of mammalian sperm, a large number of mitochondria were arranged surrounding the nucleus of newt sperm (Figure 14 B), which provided a possible platform for mitochondria-dependent cell death. Finally, it probably resulted from the specificity of this species. Without stringent controlling of early stage spermatogenic cell proliferation, the newts can firstly ensure high production of spermatids and sperm, and at the late stage of spermatogenesis, the quality of spermatids and sperm could be strictly controlled by removing abnormal spermatids and sperm via germ cell apoptosis.

Conclusion

From the results we can get several conclusions 1) p53, Apaf1, Caspase3 and Caspase7 are conserved in the testis of *Cynops orientalis*, and Caspase3, Caspase7 and Apaf1 were probably involved in the stress-triggered germ cell death while the roles played by p53 needs further investigation; 2) Spontaneous germ cell apoptosis occurred during spermatogenesis; 3) cadmium exposure, cold exposure and heat shock triggered severer apoptosis of spermatids and sperm probably both via extrinsic pathway and intrinsic pathway while starvation induced germ cell apoptosis possibly mainly via the intrinsic pathway (Figure 15).

Acknowledgments

We wish to thank the Sperm Laboratory members for many helpful discussions and Prof. Fan Jin for valuable help during the Real-Time PCR experiment.

References

- Lockshin RA, Williams CM (1964) Programmed cell death II. Endocrine potentiation of the breakdown of the intersegmental muscles of silkworms. *J Insect Physiol* 10: 643.
- Sinha Hikim AP, Swerdloff RS (1999) Hormonal and genetic control of germ cell apoptosis in the testis. *Rev Reprod* 4: 38–47.
- Sinha Hikim AP, Wang C, Lue Y, Johnson L, Wang XH, et al. (1998) Spontaneous germ cell apoptosis in humans: evidence for ethnic differences in the susceptibility of germ cells to programmed cell death. *J Clin Endocrinol Metab* 83: 152–156.
- Sinha Hikim AP, Wang C, Leung A, Swerdloff RS (1995) Involvement of apoptosis in the induction of germ cell degeneration in adult rats after gonadotropin-releasing hormone antagonist treatment. *Endocrinology* 136: 2770–2775.
- Brinkworth MH, Weinbauer GF, Schlatt S, Nieschlag E (1995) Identification of male germ cells undergoing apoptosis in adult rats. *J Reprod Fertil* 105: 25–33.
- Henriksen K, Hakovirta H, Parvinen M (1995) Testosterone inhibits and induces apoptosis in rat seminiferous tubules in a stage-specific manner: in situ quantification in squash preparations after administration of ethane dimethane sulfonate. *Endocrinology* 136: 3285–3291.
- Sinha Hikim AP, Rajavashisth TB, Sinha Hikim I, Lue Y, Bonavera JJ, et al. (1997) Significance of apoptosis in the temporal and stage-specific loss of germ cells in the adult rat after gonadotropin deprivation. *Biol Reprod* 57: 1193–1201.
- Lue Y, Hikim AP, Wang C, Bonavera JJ, Baravarian S, et al. (1997) Early effects of vasectomy on testicular structure and on germ cell and macrophage apoptosis in the hamster. *J Androl* 18: 166–173.
- Sinha Hikim AP, Lue Y, Diaz-Romero M, Yen PH, Wang C, et al. (2003) Deciphering the pathways of germ cell apoptosis in the testis. *J Steroid Biochem Mol Biol* 85: 175–182.
- Lue Y, Sinha Hikim AP, Wang C, Im M, Leung A, et al. (2000) Testicular heat exposure enhances the suppression of spermatogenesis by testosterone in rats: the “two-hit” approach to male contraceptive development. *Endocrinology* 141: 1414–1424.
- Lue YH, Hikim AP, Swerdloff RS, Im P, Taing KS, et al. (1999) Single exposure to heat induces stage-specific germ cell apoptosis in rats: role of intratesticular testosterone on stage specificity. *Endocrinology* 140: 1709–1717.
- Beumer TL, Roepers-Gajadien HL, Gademan LS, Rutgers DH, de Rooij DG (1997) P21 (Cip1/WAF1) expression in the mouse testis before and after X irradiation. *Mol Reprod Dev* 47: 240–247.
- Knudson CM, Tung KSK, Tourtellotte WG, Brown GAJ, Korsmeyer SJ (1995) Bax-deficient mice with lymphoid hyperplasia and male germ cell death. *Science* 270: 96–99.
- Furuchi T, Masuko K, Nishimune Y, Obinata M, Matsui Y (1996) Inhibition of testicular germ cell apoptosis and differentiation in mice misexpressing Bcl-2 in spermatogonia. *Development* 122: 1703–1709.
- Packer AI, Besmer P, Bachvarova RF (1995) Kit ligand mediates survival of type A spermatogonia and dividing spermatocytes in postnatal mouse testes. *Mol Reprod Dev* 42: 303–310.
- Nowicki A, Szenajch J, Ostrowska G, Wojtowicz A, Wojtowicz K, et al. (1996) Impaired tumor growth in colony-stimulating factor 1 (CSF-1)-deficient, macrophage-deficient op/op mouse: evidence for a role of CSF-1-dependent macrophages in formation of tumor stroma. *Int J Cancer* 65: 112–119.
- Richburg JH (2000) The relevance of spontaneous- and chemically-induced alterations in testicular germ cell apoptosis to toxicology. *Toxicol Lett* 112–113: 79–86.
- Gosden R, Spears N (1997) Programmed cell death in the reproductive system. *Br Med Bull* 53: 644–661.
- de Rooij DG, Grootegoed JA (1998) Spermatogonial stem cells. *Curr Opin Cell Biol* 10: 694–701.
- Matsui Y (1998) Regulation of germ cell death in mammalian gonads. *APMIS* 106: 142–147.
- Xu G, Vogel KS, McMahan CA, Herbert DC, Walter CA (2010) BAX and tumor suppressor TRP53 are important in regulating mutagenesis in spermatogenic cells in mice. *Biol Reprod* 83: 979–987.
- Ohta H, Aizawa S, Nishimune Y (2003) Functional analysis of the p53 gene in apoptosis induced by heat stress or loss of stem cell factor signaling in mouse male germ cells. *Biol Reprod* 68: 2249–2254.
- Coureuril M, Fouchet P, Prat M, Letallec B, Barroca V, et al. (2006) Caspase-independent death of meiotic and postmeiotic cells overexpressing p53: calpain involvement. *Cell Death Differ* 13: 1927–1937.
- Zou H, Henzel WJ, Liu X, Lutschg A, Wang X (1997) Apaf-1, a human protein homologous to *C. elegans* CED-4, participates in cytochrome c-dependent activation of caspase-3. *Cell* 90: 405–413.

Author Contributions

Conceived and designed the experiments: DHW JRH WXY. Performed the experiments: DHW LYW. Analyzed the data: DHW LYW YJH FQT WXY. Contributed reagents/materials/analysis tools: HZ JRH JZS YJH FQT WXY. Wrote the paper: DHW.

- Fadeel B, Ottosson A, Pervaiz S (2008) Big wheel keeps on turning: apoptosome regulation and its role in chemoresistance. *Cell Death Differ* 15: 443–452.
- Park HH, Lo YC, Lin SC, Wang L, Yang JK, et al. (2007) The death domain superfamily in intracellular signaling of apoptosis and inflammation. *Annu Rev Immunol* 25: 561–586.
- Print CG, Loveland KL (2000) Germ cell suicide: new insights into apoptosis during spermatogenesis. *Bioessays* 22: 423–430.
- Rodriguez I, Ody C, Araki K, Garcia I, Vassalli P (1997) An early and massive wave of germinal cell apoptosis is required for the development of functional spermatogenesis. *EMBO J* 16: 2262–2270.
- Krajewski S, Krajewska M, Shabaik A, Miyashita T, Wang HG, et al. (1994) Immunohistochemical determination of in vivo distribution of Bax, a dominant inhibitor of Bcl-2. *Am J Pathol* 145: 1323–1336.
- Russell LD, Chiarini-Garcia H, Korsmeyer SJ, Knudson CM (2002) Bax-dependent spermatogonia apoptosis is required for testicular development and spermatogenesis. *Biol Reprod* 66: 950–958.
- Yin Y, Stahl BC, DeWolf WC, Morgentaler A (2002) P53 and Fas are sequential mechanisms of testicular germ cell apoptosis. *J Androl* 23: 64–70.
- Lee J, Richburg JH, Younkin SC, Boekelheide K (1997) The Fas system is a key regulator of germ cell apoptosis in the testis. *Endocrinology* 138: 2081–2088.
- McClure RF, Heppelmann CJ, Paya CV (1999) Constitutive Fas ligand gene transcription in Sertoli cells is regulated by Sp1. *J Biol Chem* 274: 7756–7762.
- Young KA, Zirkin BR, Nelson RJ (1999) Short photoperiods evoke testicular apoptosis in white-footed mice (*Peromyscus leucopus*). *Endocrinology* 140: 3133–3139.
- Nandi S, Banerjee PP, Zirkin BR (1999) Germ cell apoptosis in the testes of Sprague Dawley rats following testosterone withdrawal by ethane 1,2-dimethanesulfonate administration: relationship to Fas? *Biol Reprod* 61: 70–75.
- Lee J, Richburg JH, Shipp EB, Meistrich ML, Boekelheide K (1999) The Fas system, a regulator of testicular germ cell apoptosis, is differentially up-regulated in Sertoli cell versus germ cell injury of the testis. *Endocrinology* 140: 852–858.
- Polager S, Ginsberg D (2009) p53 and E2f partners in life and death. *Nat Rev Cancer* 9: 738–748.
- Hamroun D, Kato S, Ishioka C, Claustres M, Bérout C, et al. (2006) The UMD TP53 database and website: update and revisions. *Hum Mutat* 27: 14–20.
- Beumer TL, Roepers-Gajadien HL, Gademan IS, van Buul PP, Gil-Gomez G, et al. (1998) The role of the tumor suppressor p53 in spermatogenesis. *Cell Death Differ* 5: 669–677.
- Hasegawa M, Zhang Y, Niibe H, Terry N, Meistrich M (1998) Resistance of differentiating spermatogonia to radiation-induced apoptosis and loss in p53-deficient mice. *Radiat Res* 149: 263–270.
- Allemand I, Anglo A, Jeantet AY, Cerutti I, May E (1999) Testicular wild-type p53 expression in transgenic mice induces spermiogenesis alterations ranging from differentiation defects to apoptosis. *Oncogene* 18: 6521–6530.
- Vousden KH, Prives C (2009) Blinded by the light: the growing complexity of p53. *Cell* 137: 413–431.
- Laptenko O, Prives C (2006) Transcriptional regulation by p53: one protein, many possibilities. *Cell Death Differ* 13: 951–961.
- Speidel D (2009) Transcription-independent p53 apoptosis: an alternative route to death. *Trends Cell Biol* 20: 14–24.
- Yin Y, DeWolf WC, Morgentaler A (1998) Experimental cryptorchidism induces testicular germ cell apoptosis by p53-dependent and -independent pathways in mice. *Biol Reprod* 58: 492–496.
- Yin Y, Stahl BC, DeWolf WC, Morgentaler A (1998) p53-mediated germ cell quality control in spermatogenesis. *Dev Biol* 204: 165–171.
- Ricote M, Alfaro JM, García-Tuñón I, Arenas MI, Fraile B, et al. (2002) Control of the annual testicular cycle of the marbled-newt by p53, p21, and Rb gene products. *Mol Reprod Dev* 63: 202–209.
- Yazawa T, Nakayama Y, Fujimoto K, Matsuda Y, Abe K, et al. (2003) Abnormal spermatogenesis at low temperatures in the Japanese red-bellied newt, *Cynops pyrrhogaster*: possible biological significance of the cessation of spermatocytogenesis. *Mol Reprod Dev* 66: 60–66.
- Yazawa T, Fujimoto K, Yamamoto T, Abé SI (2001) Caspase activity in newt spermatogonial apoptosis induced by prolactin and cycloheximide. *Mol Reprod Dev* 59: 209–214.
- Yazawa T, Yamamoto K, Kikuyama S, Abé SI (1999) Elevation of plasma prolactin concentrations by low temperature is the cause of spermatogonial cell death in the newt, *Cynops pyrrhogaster*. *Gen Comp Endocrinol* 103: 302–311.
- Yazawa T, Yamamoto T, Abé SI (2000) Prolactin induces apoptosis in the penultimate spermatogonial stage of the testes in Japanese red-bellied newt (*Cynops pyrrhogaster*). *Endocrinology* 141: 2027–2032.

52. Abé SI, Ji ZS (1994) Initiation and stimulation of spermatogenesis in vitro by mammalian follicle-stimulating hormone in the Japanese newt, *Cynops pyrrhogaster*. *Int J Dev Biol* 38: 201–208.
53. Yazawa T, Yamamoto T, Kubokawa K, Nakayama Y, Fujimoto K, et al. (2001) Cold suppression of follicle-stimulating hormone activity on proliferation and survival of newt spermatogonia. *Gen Comp Endocrinol* 122: 296–303.
54. Kim MS, Kim BJ, Woo HN, Kim KW, Kim KB, et al. (2000) Cadmium induces caspase-mediated cell death: suppression by Bcl-2. *Toxicology* 145: 27–37.
55. Roy A, Kucukural A, Zhang Y (2010) I-TASSER: a unified platform for automated protein structure and function prediction. *Nat Protoc* 5: 725–738.
56. Roy A, Xu D, Poisson J, Zhang Y (2011) A protocol for computer-based protein structure and function prediction. *J Vis Exp* 3: e3259.
57. Zhang Y (2008) I-TASSER server for protein 3D structure prediction. *BMC Bioinformatics* 9: 40.
58. Ho WC, Fitzgerald MX, Marmorstein R (2006) Structure of the p53 core domain dimer bound to DNA. *J Biol Chem* 281: 20494–20502.
59. Gordo S, Martos V, Santos E, Menéndez M, Bo C, et al. (2008) Stability and structural recovery of the tetramerization domain of p53-R337H mutant induced by a designed templating ligand. *Proc Natl Acad Sci U S A* 105: 16426–16431.
60. Qin H, Srinivasula SM, Wu G, Fernandes-Alnemri T, Alnemri ES, et al. (1999) Structural basis of procaspase-9 recruitment by the apoptotic protease-activating factor 1. *Nature* 399: 549–557.
61. Yu X, Acehan D, Ménétret JF, Booth CR, Ludtke SJ, et al. (2005) A structure of the human apoptosome at 12.8 Å resolution provides insights into this cell death platform. *Structure* 13: 1725–1735.
62. Riedl SJ, Salvesen GS (2007) The apoptosome: signaling platform of cell death. *Nat Rev Mol Cell Biol* 8: 405–413.
63. Yuan S, Yu X, Topf M, Ludtke SJ, Wang X, et al. (2010) Structure of an apoptosome-procaspase-9 CARD complex. *Structure* 18: 571–583.
64. Reubold TF, Wohlgenuth S, Eschenburg S (2011) Crystal structure of full-length Apaf-1: how the death signal is relayed in the mitochondrial pathway of apoptosis. *Structure* 19: 1074–1083.
65. Li M, Ding Y, Mu Y, Ao J, Chen X (2011) Molecular cloning and characterization of caspase-3 in large yellow croaker (*Pseudosciaena crocea*). *Fish Shellfish Immunol* 30: 910–916.
66. Yan N, Shi Y (2005) Mechanisms of apoptosis through structural biology. *Annu Rev Cell Dev Biol* 21: 35–56.
67. Riedl SJ, Renatus M, Schwarzenbacher R, Zhou Q, Sun C, et al. (2001) Structural basis for the inhibition of caspase-3 by XIAP. *Cell* 104: 791–800.
68. Ekert PG, Vaux DL (2005) The mitochondrial death squad: hardened killers or innocent bystanders? *Curr Opin Cell Biol* 17: 626–30.
69. Honarpour N, Du C, Richardson JA, Hammer RE, Wang X, et al. (2000) Adult Apaf-1-deficient mice exhibit male infertility. *Dev Biol* 218: 248–58.
70. Honarpour N, Du C, Richardson JA, Hammer RE, Wang X, et al. (2000) Adult Apaf-1-deficient mice exhibit male infertility. *Dev Biol* 218: 248–58.
71. Salazar G, Joshi A, Liu D, Wei H, Persson JL, et al. (2005) Induction of apoptosis involving multiple pathways is a primary response to cyclin A1-deficiency in male meiosis. *Dev Dyn* 234: 114–123.
72. Wolgemuth DJ (2003) Insights into regulation of the mammalian cell cycle from studies on spermatogenesis using genetic approaches in animal models. *Cytogenet Genome Res* 103: 256–266.
73. Lee S, Elenbaas B, Levine A, Griffith J (1995) p53 and its 14 kDa C-terminal domain recognize primary DNA damage in the form of insertion/deletion mismatches. *Cell* 81: 1013–1020.
74. Oberosler P, Hloch P, Ramsperger U, Stahl H (1993) p53-catalyzed annealing of complementary single-stranded nucleic acids. *EMBO J* 12: 2389–2396.
75. Bakalkin G, Yakovleva T, Selivanova G, Magnusson KP, Szekely L, et al. (1994) p53 binds single-stranded DNA ends and catalyzes DNA renaturation and strand transfer. *Proc Natl Acad Sci USA* 91: 413–417.
76. Said TM, Paasch U, Glander HJ, Agarwal A (2004) Role of caspases in male infertility. *Hum Reprod Update* 10: 39–51.
77. Wang Q, Zhao XF, Ji YL, Wang H, Liu P, et al. (2010) Mitochondrial signaling pathway is also involved in bisphenol A induced germ cell apoptosis in testes. *Toxicol Lett* 199: 129–135.
78. Bartke A (1995) Apoptosis of male germ cells, a generalized or a cell type-specific phenomenon? *Endocrinology* 36: 3–4.
79. Billig H, Furuka I, Rivier C, Tapanainen J, Parvinen M, et al. (1995) Apoptosis in testis germ cells: developmental changes in gonadotropin dependence and localization to selective tubule stages. *Endocrinology* 136: 5–12.
80. Sen Gupta R, Kim J, Gomes C, Oh S, Park J, et al. (2004) Effect of ascorbic acid supplementation on testicular steroidogenesis and germ cell death in cadmium-treated male rats. *Mol Cell Endocrinol* 221: 57–66.
81. Vera Y, Erkkilä K, Wang C, Nunez C, Kytönen S, et al. (2006) Involvement of p38 mitogen-activated protein kinase and inducible nitric oxide synthase in apoptotic signaling of murine and human male germ cells after hormone deprivation. *Mol Endocrinol* 20: 1597–1609.
82. Embree-Ku M, Venturini D, Boeckelheide K (2002) Fas is involved in the p53-dependent apoptotic response to ionizing radiation in mouse testis. *Biol Reprod* 66: 1456–1461.
83. Chai J, Shiozaki E, Srinivasula SM, Wu Q, Datta P, et al. (2001) Structural basis of caspase-7 inhibition by XIAP. *Cell* 104: 769–780.
84. Hueber AO, Zornig M, Lyon D, Suda T, Nagata S, et al. (1997) Requirement for the CD95 receptor-ligand pathway in c-Myc-induced apoptosis. *Science* 278: 1305–1309.
85. Schamberger CJ, Gerner C, Cerni C (2005) Caspase-9 plays a marginal role in serum starvation-induced apoptosis. *Exp Cell Res* 302: 115–28.
86. Rathmell JC, Fox CJ, Plas DR, Hammerman PS, Cinalli RM, et al. (2003) Akt-directed glucose metabolism can prevent Bax conformation change and promote growth factor-independent survival. *Mol Cell Biol* 23: 7315–7328.
87. Zhao Y, Altman BJ, Colloff JL, Herman CE, Jacobs SR, et al. (2007) Glycogen synthase kinase 3alpha and 3beta mediate a glucose-sensitive antiapoptotic signaling pathway to stabilize Mcl-1. *Mol Cell Biol* 27: 4328–4339.
88. Zhao Y, Colloff JL, Ferguson EC, Jacobs SR, Cui K, et al. (2008) Glucose metabolism attenuates p53 and Puma-dependent cell death upon growth factor deprivation. *J Biol Chem* 283: 36344–36353.
89. Lomb DJ, Desouza LA, Franklin JL, Freeman RS (2009) Prolyl hydroxylase inhibitors depend on extracellular glucose and hypoxia-inducible factor (HIF)-2alpha to inhibit cell death caused by nerve growth factor (NGF) deprivation: evidence that HIF-2alpha has a role in NGF-promoted survival of sympathetic neurons. *Mol Pharmacol* 75: 1198–1209.
90. Morissette MR, Howes AL, Zhang T, Heller Brown J (2003) Upregulation of GLUT1 expression is necessary for hypertrophy and survival of neonatal rat cardiomyocytes. *J Mol Cell Cardiol* 35: 1217–1227.
91. Hall JL, Chatham JC, Eldar-Finkelman H, Gibbons GH (2001) Upregulation of glucose metabolism during intimal lesion formation is coupled to the inhibition of vascular smooth muscle cell apoptosis. Role of GSK3beta. *Diabetes* 50: 1171–1179.
92. Vander Heiden MG, Plas DR, Rathmell JC, Fox CJ, Harris MH, et al. (2001) Growth factors can influence cell growth and survival through effects on glucose metabolism. *Mol Cell Biol* 21: 5899–5912.
93. Mason EF, Rathmell JC (2011) Cell metabolism: an essential link between cell growth and apoptosis. *Biochim Biophys Acta* 1813: 645–654.
94. Kaufmann SH, Hengartner MO (2001) Programmed cell death: alive and well in the new millennium. *Trends Cell Biol* 11: 526–534.
95. Allsopp TE, McLuckie J, Kerr LE, Macleod M, Sharkey J, et al. (2000) Caspase 6 activity initiates caspase 3 activation in cerebellar granule cell apoptosis. *Cell Death Differ* 7: 984–993.
96. Kilic M, Schafer R, Hoppe J, Kagerhuber U (2002) Formation of noncanonical high molecular weight caspase-3 and -6 complexes and activation of caspase-12 during serum starvation induced apoptosis in AKR-2B mouse fibroblasts. *Cell Death Differ* 9: 125–137.
97. Chipuk JE, Green DR (2008) How do BCL-2 proteins induce mitochondrial outer membrane permeabilization? *Trends Cell Biol* 18: 157–164.
98. Ekert PG, Read SH, Silke J, Marsden VS, Kaufmann H, et al. (2004) Apaf-1 and caspase-9 accelerate apoptosis, but do not determine whether factor-deprived or drug-treated cells die. *J Cell Biol* 165: 835–842.
99. Canman CE, Gilmer TM, Coutts SB, Kastan MB (1995) Growth factor modulation of p53-mediated growth arrest versus apoptosis. *Genes Dev* 9: 600–11.
100. Thangaraju M, Kaufmann SH, Couch FJ (2000) BRCA1 facilitates stress-induced apoptosis in breast and ovarian cancer cell lines. *J Biol Chem* 275: 33487–33496.
101. Zhou T, Zhou G, Song W, Eguchi N, Lu W, et al. (1999) Cadmium-induced apoptosis and changes in expression of p53, c-jun and MT-I genes in testes and ventral prostate of rats. *Toxicology* 142: 1–13.
102. Siu ER, Mruk DD, Porto CS, Cheng CY (2009) Cadmium-induced testicular injury. *Toxicol Appl Pharmacol* 238: 240–249.
103. Ozawa N, Goda N, Makino N, Yamaguchi T, Yoshimura Y, et al. (2002) Leydig cell-derived heme oxygenase-1 regulates apoptosis of premeiotic germ cells in response to stress. *J Clin Invest* 109: 457–467.
104. Pant N, Upadhyay G, Pandey S, Mathur N, Saxena DK, et al. (2003) Lead and cadmium concentration in the seminal plasma of men in the general population: correlation with sperm quality. *Reprod Toxicol* 17: 447–450.
105. Kim J, Soh J (2009) Cadmium-induced apoptosis is mediated by the translocation of AIF to the nucleus in rat testes. *Toxicol Lett* 188: 45–51.
106. Xu C, Johnson JE, Singh PK, Jones MM, Yan H, et al. (1996) In vivo studies of cadmium-induced apoptosis in testicular tissue of the rat and its modulation by a chelating agent. *Toxicology* 107: 1–8.
107. Ji YL, Wang H, Liu P, Wang Q, Zhao XF, et al. (2010) Pubertal cadmium exposure impairs testicular development and spermatogenesis via disrupting testicular testosterone synthesis in adult mice. *Reprod Toxicol* 29: 176–183.
108. Lafuente A, Cano P, Esquifino A (2003) Are cadmium effects on plasma gonadotropins, prolactin, ACTH, GH and TSH levels, dose-dependent? *Biometals* 16: 243–250.
109. Lafuente A, González-Carracedo A, Romero A, Cano P, Esquifino AI (2004) Cadmium exposure differentially modifies the circadian patterns of norepinephrine at the median eminence and plasma LH, FSH and testosterone levels. *Toxicol Lett* 146: 175–182.
110. Laskey JW, Phelps PV (1991) Effect of cadmium and other metal cations on in vitro Leydig cell testosterone production. *Toxicol Appl Pharmacol* 108: 296–306.
111. Ragan HA, Mast TJ (1990) Cadmium inhalation and male reproductive toxicology. *Rev Environ Contam Toxicol* 114: 1–22.
112. Hew KW, Ericson WA, Welsh MJ (1993) A single low cadmium dose causes failure of spermiogenesis in the rat. *Toxicol Appl Pharmacol* 121: 15–21.

113. Yang JM, Arnush M, Chen QY, Wu XD, Pang B, et al. (2003) Cadmium-induced damage to primary cultures of rat Leydig cells. *Reprod Toxicol* 142: 553–560.
114. Roberts KP, Zirkin BR (1991) Androgen regulation of spermatogenesis in the rat. *Ann N Y Acad Sci* 637: 90–106.
115. O'Donnell L, McLachlan RI, Wreford NG, de Kretser DM, Robertson DM (1996) Testosterone withdrawal promotes stage-specific detachment of round spermatids from the rat seminiferous epithelium. *Biol Reprod* 55: 895–901.
116. Pareek TK, Joshi AR, Sanyal A, Dighe RR (2007) Insights into male germ cell apoptosis due to depletion of gonadotropins caused by GnRH antagonists. *Apoptosis* 12: 1085–1100.
117. Woolveridge I, Boer-Brouwer M, Taylor MF, Teerds KJ, Wu FCW, et al. (1999) Apoptosis in the rat spermatogenic epithelium following androgen withdrawal: changes in apoptosis-related genes. *Biol Reprod* 60: 461–470.
118. Stocco DM, Wells J, Clark BJ (1993) The effects of hydrogen peroxide on steroidogenesis in mouse Leydig tumor cells. *Endocrinology* 133: 2827–2832.
119. Ciesielska AS, Stachura A, Slotwinska M, Kaminska T, Sniezko R, et al. (2000) The inhibitory effect of zinc on cadmium-induced cell apoptosis and reactive oxygen species production in cell culture. *Toxicology* 145: 171–183.
120. Stohs SJ, Bagchi D, Hassoun E, Bagchi M (2001) Oxidative mechanism in toxicity of chromium and cadmium ions. *J Environ Pathol Oncol* 20: 77–88.
121. Jimi S, Uchiyama M, Takaki A, Suzumiya J, Hara S (2004) Mechanisms of cell death induced by cadmium and arsenic. *Ann N Y Acad Sci* 1011: 325–331.
122. Liu J, Shen HM, Ong CN (2001) Role of intracellular thio depletion, mitochondrial dysfunction and reactive oxygen species in *Salvia miltiorrhiza*-induced apoptosis in human hepatoma HepG2 cells. *Life Sci* 69: 1833–1850.
123. Hassoun EA, Stohs SJ (1996) Cadmium-induced production of superoxide and nitric oxide. DNA single strand breaks and lactate dehydrogenase leakage in J774A.1 cell cultures. *Toxicology* 112: 219–226.
124. Wu X, Faqi AS, Yang J, Pang B, Ding X, et al. (2002) 2-Bromopropane induces DNA damage, impairs functional antioxidant cellular defenses, and enhances the lipid peroxidation process in primary cultures of rat Leydig cells. *Reprod Toxicol* 16: 379–384.
125. Bonini P, Cicconi S, Cardinale A, Vitale C, Serafino AL, et al. (2004) Oxidative stress induces p53-mediated apoptosis in glia: p53 transcription-independent way to die. *J Neurosci Res* 75: 83–95.
126. Kasahara E, Sato EF, Miyoshi M, Konaka R, Hiramoto K, et al. (2002) Role of oxidative stress in germ cell apoptosis induced by di (2-ethylhexyl) phthalate. *Biochem J* 365: 849–856.
127. Kondoh M, Araragi S, Sato K, Higashimoto M, Takiguchi M, et al. (2002) Cadmium induces apoptosis partly via caspase-9 activation in HL-60 cells. *Toxicology* 170: 111–117.
128. Li M, Kondo T, Zhao QL, Li FJ, Tanabe K, et al. (2000) Apoptosis induced by cadmium in human lymphoma U937 cells through Ca²⁺-calpain and caspase-mitochondria-dependent pathways. *J Biol Chem* 275: 39702–39709.
129. Vousden KH (2006) Outcomes of p53 activation—spoils for choice. *J Cell Sci* 19: 5015–20.
130. Zheng H, Liu J, Choo KHA, Michalska AE, Klaassen CD (1996) Metallothionein-I and -II knock-out mice are sensitive to cadmium-induced liver mRNA expression of c-jun and p53. *Toxicol Appl Pharmacol* 136: 229–235.
131. Mieuisset R, Bujan L (1995) Testicular heating and its possible contributions to male fertility: a review. *Int J Androl* 18: 169–184.
132. Chowdhury AK, Steinberger E (1964) A quantitative study of the effect of heat on germinal epithelium of rat testes. *J Anat* 115: 509–524.
133. Vera Y, Diaz-Romero M, Rodriguez S, Lue Y, Wang C, et al. (2004) Mitochondria-dependent pathway is involved in heat induced male germ cell death: lessons from mutant mice. *Biol Reprod* 70: 1534–1540.
134. Bernal-Mañas CM, Morales E, Pastor LM, Pinart E, Bonet S, et al. (2005) Proliferation and apoptosis of spermatogonia in postpubertal boar (*Sus domesticus*) testes with spontaneous unilateral and bilateral abdominal cryptorchidism. *Acta Histochem* 107: 365–372.
135. Xu J, Xu Z, Jiang Y, Qian X, Huang Y (2000) Cryptorchidism induces mouse testicular germ cell apoptosis and changes in bcl-2 and bax protein expression. *J Environ Pathol Toxicol Oncol* 19: 25–33.
136. Zhang ZH, Jin X, Zhang XS, Hu ZY, Zou RJ, et al. (2003) Bcl-2 and Bax are involved in experimental cryptorchidism-induced testicular germ cell apoptosis in rhesus monkeys. *Contraception* 68: 297–301.
137. Heckert L, Griswold MD (1993) Expression of the FSH receptor in the testis. *Recent Prog Horm Res* 48: 61–77.
138. Ji ZS, Abé S (1994) Mammalian follicle-stimulating hormone stimulates DNA synthesis in secondary spermatogonia and Sertoli cells in organ culture of testes fragments from the newt, *Cynops pyrrhogaster*. *Zygote* 2: 53–61.
139. Huang Y, Jin H, Liu Y, Zhou J, Ding J, et al. (2010) FSH inhibits ovarian cancer cell apoptosis by up-regulating Survivin and down-regulating PDCD6 and DR5. *Endocr Relat Cancer* 18: 13–26.
140. Blanco-Rodriguez J, Martinez-Garcia C, Porras A (2003) Correlation between DNA synthesis in the second, third and fourth generations of spermatogonia and the occurrence of apoptosis in both spermatogonia and spermatocytes. *Reproduction* 126: 661–668.
141. Li LH, Wine RN, Chapin RE (1996) 2-Methoxyacetic acid (MAA)-induced spermatocyte apoptosis in human and rat testes: an in vitro comparison. *J Androl* 17: 538–548.
142. Huckins C (1978) The morphology and kinetics of spermatogonial degeneration in normal adult rats: An analysis using a simplified classification of the germinal epithelium. *Anat Rec* 190: 905–926.
143. Allan DJ, Harmon BV, Roberts SA (1992) Spermatogonia apoptosis has three morphologically recognizable phases and shows no circadian rhythm during normal spermatogenesis in the rat. *Cell Prolif* 25: 241–250.
144. Paasch U, Grunewald S, Fitzl G, Glander H (2003) Deterioration of plasma membrane is associated with activated caspases in human spermatozoa. *J Androl* 24: 246–252.
145. Thornberry N, Lazebnik Y (1998) Caspases: enemies within. *Science* 281: 1312–1316.
146. Paasch U, Grunewald S, Glander HJ (2002) Presence of up- and downstream caspases in relation to impairment of human spermatogenesis. *Andrologia* 34: 279.
147. Weng S, Taylor S, Morshedi M, Schuffner A, Duran E, et al. (2002) Caspase activity and apoptotic markers in ejaculated human sperm. *Mol Hum Reprod* 8: 984–991.
148. Wang X, Sharma R, Sikka S, Thomas AJ Jr, Falcone T, et al. (2003) Oxidative stress is associated with increased apoptosis leading to spermatozoa DNA damage in patients with male factor infertility. *Fertil Steril* 80: 531–535.